Proving chaos for a system of coupled logistic maps: a topological approach

A. Bosisio,[1, a)] A. Naimzada,[2] and M. Pireddu[3]

[1)]*Sempione Sim SPA, Via Maurizio Gonzaga 2, 20123 Milano, Italy*

[2)]*Dept. of Economics, Management and Statistics, University of Milano - Bicocca, U6 Building, Piazza dell'Ateneo Nuovo 1, 20126 Milano, Italy*

[3)]*Dept. of Mathematics and its Applications, University of Milano - Bicocca, U5 Building, Via R. Cozzi 55, 20125 Milano, Italy*

(*Electronic mail: marina.pireddu@unimib.it)

(*Electronic mail: ahmad.naimzada@unimib.it)

(*Electronic mail: alessio.bosisio@tiscali.it)

(Dated: 31 January 2024)

In the work we prove the presence of chaotic dynamics, for suitable values of the model parameters, for the discrete-time system, composed of two coupled logistic maps, as formulated in Yousefi et al. [Discrete Dyn. Nat. Soc. **5**, 161–177 (2000)] and describing two interdependent economies, characterized by two competitive markets each, with a demand link between them. In particular, we rely on the SAP (Stretching Along the Paths) method, based on a stretching relation for maps defined on sets homeomorphic to the unit square and expanding the paths along one direction. Such technique is topological in nature and allows to establish the existence of a semiconjugacy between the considered dynamical system and the Bernoulli shift, so that the main features related to chaos of the latter (e.g., the positivity of the topological entropy) are transmitted to the former. In more detail, we apply the SAP method both to the first and to the second iterate of the map associated with our system and we show how dealing with the second iterate, although being more demanding in terms of computations, allows for a larger freedom in the sign and in the variation range of the linking parameters for which chaos emerges. Moreover, the latter choice guarantees a good agreement with the numerical simulations, that highlight the presence of a chaotic attractor under the conditions derived for the applicability of the SAP technique to the second iterate of the map.

[a)]Past position: Master Degree in Mathematics, University of Milano - Bicocca

In the manuscript we rigorously prove the presence of complex dynamics for the coupled logistic map, as formulated in[1], by means of the Stretching Along the Paths (henceforth, SAP) method, which is a topological technique that has been developed in the planar case in[2,3] and then extended to the N-dimensional framework, with $N \geq 3$, in[4]. Despite in the Introduction of[1] Yousefi et al., referring to their system composed of two logistic maps, coupled by linear terms, say that "*To the best of our knowledge, so far, this kind of system has not been subjected to mathematical investigations at an advanced level. Any such investigation must incorporate two different aspects, namely the global dynamics of diffeomorphisms and the theory of critical lines developed in Mira et al.***[5]**", we here follow, in view of showing the presence of chaos in that setting, a different approach which, being topological in nature, does not require any differentiability condition. Moreover, the SAP technique has proven to be successfully applicable both in discrete-[6–8] and in continuous-time contexts (see e.g.[9–11]). The versatility of the SAP method comes from the fact that it does not call for a direct proof of chaos according to one of the many existing definitions, which are often difficult, or impossible to handle in practical contexts. Namely, the SAP technique, in agreement with a canonical strategy in the chaos literature (cf. for instance[12,13]), allows to establish a semiconjugacy between the function under investigation, or one of its iterates, and the Bernoulli shift on two (or more) symbols, which displays many chaotic features, such as topological transitivity, sensitivity on initial conditions and positive topological entropy. In that indirect manner, it is possible to conclude that the considered dynamical system satisfies all the properties of the Bernoulli shift that are preserved by the semiconjugacy relation. This is the strategy that we shall employ along the manuscript, where, after determining the parameter conditions that ensure the emergence of chaotic dynamics when applying the SAP method to the first iterate of the map associated with the system considered in[1], we apply the SAP method to the second iterate of the same map in order to weaken those conditions, both in regard to the sign and the variation range of the parameters involved. Furthermore, the application of the SAP method to the second iterate of the map generating the dynamics allows us to obtain a good agreement with the numerical simulations, that confirm the presence of a chaotic attractor under the conditions derived for the applicability of the SAP technique to the second iterate of the map, but not to the first iterate, in which case chaotic sets are not attractive. To the best of our knowledge, the one we provide is the first discrete-time application of the SAP technique in which numerical simulations highlight the presence of a chaotic attractor.**

I. INTRODUCTION

The present work aims at providing a topological proof of the existence of chaotic dynamics for the discrete-time system composed of two coupled logistic maps, according to the formulation given in[1], which describes two interdependent economies, characterized by two competitive markets each, with a demand link between them.

Indeed, our study belongs to the vast literature that, starting from the 80s, investigates via simulative (see e.g.[14–16]) or analytical (cf. for instance[17]) methods the dynamic effect of various, linear or nonlinear, coupling formulations between two or more logistic maps.[18] The study of coupled logistic maps went on in the past decades (see e.g.[19–23]) and still in very recent times many authors have been dealing with such topic, either in its simplest form encompassing just two functions, for instance in order to study, mainly by means of analytical tools, its bifurcations, like done in[24,25], as well as in[26,27] in the presence of noise, or in more complex versions, encompassing noise signals and networks, like in[28–30], mostly from a numerical viewpoint. In agreement with the former, more theoretical literature strand, in this work we rigorously prove the presence of complex dynamics for the coupled logistic map, as formulated in[1], by means of the Stretching Along the Paths (henceforth, SAP) method, which is a topological technique that has been developed in the planar case in[2,3] and then extended to the N-dimensional framework, with $N \geq 3$, in[4]. It allows to detect the existence of fixed points, periodic points, and chaos for maps for which it is known, or for which it is possible to show, that they are expansive (thus stretching the paths) along one direction and contractive along the remaining $N-1$ directions, being defined on subsets of $\mathbb{R}^N$ homeomorphic to the N-dimensional cube, which we will call generalized rectangles for $N = 2$. In the planar case, the SAP method consists in finding a generalized rectangle which, when appropriately oriented by choosing two disjoint arcs in its boundary, contains at least two disjoint compact subsets on which a suitable stretching relation is fulfilled between the generalized rectangle *and itself*, while keeping its orientation unchanged, so that the generalized rectangle is stretched at least twice across itself by the considered map. The possibility of detecting, by means of analytical conditions, such a generalized rectangle depends on the geometry associated with the iterates of the map governing the dynamics, and in particular on the way in which sets are deformed by its forward iterates. Namely, this task turns out to be easy when the function under consideration produces a stretching

and a folding on some set similar to that impressed by the original Smale Horseshoe in[31] on the unit square (see also Ch. 23 in[32] for a detailed construction and description of the features for a simplified version of it).[33]

Starting from[2,3], the SAP method has been used both in discrete- and continuous-time models. In the latter case, a field of application is given by Hamiltonian systems with a nonisochronous center in which it is sensible to assume a periodic variation in some of the model coefficients, so as to enter the geometrical framework of "Linked Twist Maps" (henceforth, LTMs), where the SAP method is applied to the Poincaré map associated with the considered system, and this leads again to the study of a discrete-time setting. We refer the interested reader e.g. to[9–11,34–36] for continuous-time planar applications of the SAP method, and to[37,38] for 3D continuous-time applications of it to non-Hamiltonian systems. On the other hand, to the best of our knowledge, the only applications of the SAP technique to discrete-time models can be found in[6–8], where 1D[39], 2D (in[6]) and 3D (in[7,8]) economic settings are considered. In more detail, in[7,8] different triopoly game models with heterogeneous players, taken respectively from[40] and[41,42], are analyzed, while in[6] OLG models with and without production (taken e.g. from[43,44]), as well as the duopoly game model with heterogeneous players taken from[45], are considered.

Following the approach employed in[6–8], along the manuscript we show how to apply the SAP method to the model in[1] so as to detect chaotic dynamics therein. In particular, the possibility of finding a generalized rectangle for which the stretching relation is satisfied with respect to two disjoint compact subsets of it depends, in addition to the value assumed by the usual parameter present in the two logistic maps, on the sign and on the value of the parameters describing the link between the two economies. Specifically, when dealing with the first iterate of the map generating the dynamics, we obtain that the SAP method can be applied only when one of the linking parameters is negative. In order to overcome such limitation, we also consider the second iterate of the same map and we show that applying the SAP method to it, although being more demanding in terms of computations, allows for a larger freedom in the sign and in the variability range of the linking parameters for which chaos emerges. In addition to this, the application of the SAP method to the second iterate of the map generating the dynamics guarantees a good agreement with the numerical simulations, that confirm the presence of a chaotic attractor under the conditions derived for the applicability of the SAP technique to the second iterate of the map, but not to the first iterate, in which case chaotic sets are not attractive. Namely, in general the SAP method ensures the existence of chaotic sets, but not their attractiveness, as discussed in[6].

To the best of our knowledge, the one provided here is the first application of the SAP technique to a discrete-time framework in which numerical simulations highlight the presence of a chaotic attractor, thanks to the careful way in which our method is employed, justifying the cumbersome computations involved.

We finally stress that the analysis we shall perform and the kind of obtained results would be valid also when investigating the analogous system composed of three coupled logistic maps. In more detail, in order to have the stretching relation, on which the SAP method is based, satisfied requires to assume that there are, for the function associated with the 3D system, two compressive directions and that the third one is expansive. However, in order not to overburden the paper, we prefer to focus on the planar framework only, making just some remarks along the manuscript on how our findings would look like in the three-dimensional setting, also by means of a few illustrations, which confirm the presence of a chaotic attractor when the SAP method is applicable to prove the existence of chaotic sets for the second iterate of the function associated with the three-dimensional dynamical system.

The remainder of the paper is organized as follows. In Sec. II we recall the main definitions and results connected with the SAP method. In Sec. III we briefly introduce the model that we are going to analyze. In Sec. IV we show how to apply the SAP method to the first iterate of the map generating the dynamics. In Sec. V we explain how to apply the SAP technique to the second iterate. In Sec. VI we conclude.

II. RECALLING THE STRETCHING ALONG THE PATHS METHOD

The Stretching Along the Paths (henceforth, SAP) method is a topological technique that allows to detect the existence of chaotic dynamics for maps, defined on subsets of $\mathbb{R}^N$ homeomorphic to the N-dimensional cube, for which it is known, or it is possible to show, that they are expansive along one direction and contractive along the remaining $N-1$ directions. It has been developed in the planar case in[2,3] and extended in[4] to the N-dimensional framework, with $N \geq 3$. The SAP method, which is based on the stretching relation in Definition II.1 below and on its properties, has been applied both to discrete-time (cf.[6–8]) and to continuous-time (see e.g.[9,34,35,37,38]) 2D and 3D systems.

For brevity's sake, in what follows we recall just the definitions and the results about the SAP relation that are needed in view of some remarks about the related literature, and that we will use

in our applications in Sec. IV and in Sec. V, focusing on the 2D framework. Further details and more general planar formulations can be found e.g. in[46,47]. We will make some comments about the 1D setting at the end of the present section, while we refer the reader to[8] for the theoretical results in the 3D framework, since along the paper the three-dimensional model will be considered just in a marginal way.

A *path* in $\mathbb{R}^2$ is a continuous map $\gamma : [t_0, t_1] \to \mathbb{R}^2$, for some $t_0 < t_1$. Without loss of generality, we usually take the unit interval $[0,1]$ as domain of γ, and we denote by $\overline{\gamma} := \gamma([0,1])$ its image. A subpath ν of γ is the restriction of γ to a compact subinterval of its domain. A *generalized rectangle* is a subset $\mathscr{R}$ of $\mathbb{R}^2$ which is homeomorphic to the unit square $[0,1]^2$ through a homeomorphism $H : \mathbb{R}^2 \supseteq [0,1]^2 \to \mathscr{R} \subseteq \mathbb{R}^2$. A generalized rectangle is oriented by choosing two disjoint arcs in its boundary, that will be named left and right sides of the generalized rectangle. Indeed, we call $\mathscr{R}_\ell^- := H(\{0\} \times [0,1])$ the *left side* of $\mathscr{R}$ and $\mathscr{R}_r^- := H(\{1\} \times [0,1])$ its *right side* and an *oriented rectangle of* $\mathbb{R}^2$ is a pair $\widetilde{\mathscr{R}} := (\mathscr{R}, \mathscr{R}^-)$, where $\mathscr{R}$ is a generalized rectangle and $\mathscr{R}^- := \mathscr{R}_\ell^- \cup \mathscr{R}_r^-$. Moreover, we call $\mathscr{R}_d^+ := H([0,1] \times \{0\})$ the *down side* of $\mathscr{R}$ and $\mathscr{R}_u^+ := H([0,1] \times \{1\})$ its *up side*.[48]

The *stretching along the paths* (SAP) relation for maps between oriented rectangles is recalled in the following:

Definition II.1 *Given the oriented rectangles* $\widetilde{\mathscr{A}} := (\mathscr{A}, \mathscr{A}^-)$ *and* $\widetilde{\mathscr{B}} := (\mathscr{B}, \mathscr{B}^-)$ *of* $\mathbb{R}^2$, *let* $K \subseteq \mathscr{A}$ *be a compact set and* $F : \mathscr{A} \to \mathbb{R}^2$ *be a function. We say that*

$$(K,F) \text{ stretches } \widetilde{\mathscr{A}} \text{ to } \widetilde{\mathscr{B}} \text{ along the paths,}$$

and write

$$(K,F) : \widetilde{\mathscr{A}} \twoheadrightarrow \widetilde{\mathscr{B}}, \tag{2.1}$$

if it holds that:

- F *is continuous on* K;
- *for every path* $\gamma : [0,1] \to \mathscr{A}$ *with* $\gamma(0)$ *and* $\gamma(1)$ *belonging to the different components of* $\mathscr{A}^-$, *there exists* $[t', t''] \subseteq [0,1]$ *such that* $\gamma([t', t'']) \subseteq K$ *and* $F(\gamma([t', t''])) \subseteq \mathscr{B}$, *with* $F(\gamma(t'))$ *and* $F(\gamma(t''))$ *belonging to the different components of* $\mathscr{B}^-$.

Thanks to Lemma 2.11 in[46], when the SAP relation in (2.1) is fulfilled, there exists a compact, connected set C contained in K and joining $\mathscr{A}_d^+$ to $\mathscr{A}_u^+$ (see Fig. 1 for a graphical illustration, where, for simplicity's sake, we let C coincide with K).

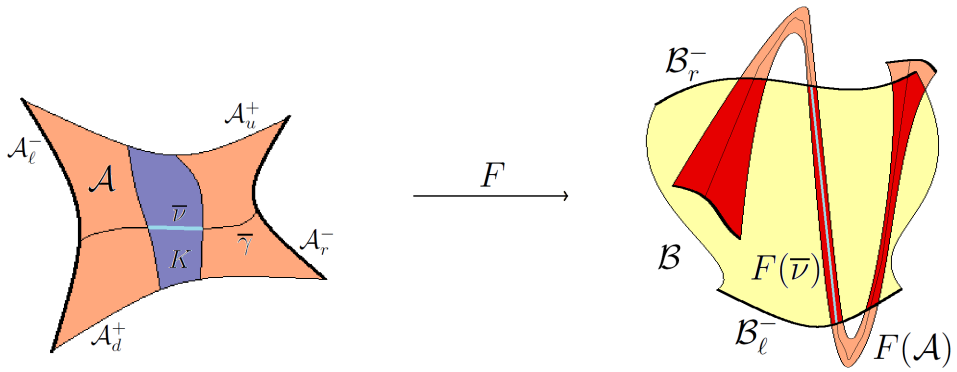

FIG. 1. We illustrate the stretching relation $(K,F) : \widetilde{\mathscr{A}} \twoheadrightarrow \widetilde{\mathscr{B}}$ between the generalized rectangles $\widetilde{\mathscr{A}} := (\mathscr{A}, \mathscr{A}^-)$ and $\widetilde{\mathscr{B}} := (\mathscr{B}, \mathscr{B}^-)$. We use the same color to draw an object in $\mathscr{A}$ (on the left) and its image through F (on the right). In particular, given the generic path γ joining the left and the right sides of $\mathscr{A}$, we draw in light blue its subpath ν in K, whose image through F, still colored in light blue, joins the boundary sets $\mathscr{B}_\ell^-$ and $\mathscr{B}_r^-$ of $\mathscr{B}$.

Moreover, according to Theorem 2.1 in[6], when the stretching relation in (2.1) is satisfied with $\widetilde{\mathscr{A}} = \widetilde{\mathscr{B}}$, so that $\mathscr{A} = \mathscr{B}$ and the orientation of the two generalized rectangles coincides, too, a fixed point localized in the compact set K exists. Under the same assumptions, since the stretching relation is preserved under composition of maps (see Lemma 2.2 in[47]), dealing with the forward iterates of a function allows to show the existence of periodic points of any period.[49] We further stress that, despite the similarity between the SAP relation and the crossing property by Kennedy and Yorke in[13], where connections and preconnections play the role of our paths and subpaths, the latter approach, also due to the generality of the spaces considered, does not guarantee the existence of fixed points and periodic points when the crossing property in[13] is fulfilled between a domain and itself, as shown by Example 10 therein. In particular, such difference affects the definition of chaos that it is possible to deal with by using the two methods. Indeed, under the assumptions of Theorem II.1, in agreement with points (ii) and (iii) of that result, rather than the classical characterization of chaos in the coin-tossing sense by Kirchgraber and Stoffer in[50] - considered also, among others, in[13,51] - according to which the iterates of the map generating the system dynamics mimic the sequences of two symbols, we can also require that periodic sequences of symbols are realized by means of periodic itineraries of the map. See[6], and in particular Definition 2.2 and the proof of Theorem 2.2 therein, for additional details.

Furthermore, notice that if it holds that $(K,F) : \widetilde{\mathscr{A}} \twoheadrightarrow \widetilde{\mathscr{B}}$ for some $K \subset \mathscr{A}$ and F is continuous on

$\mathscr{A}$, then it is true that $(\mathscr{A},F):\widetilde{\mathscr{A}}\overset{\sim}{\Rightarrow}\widetilde{\mathscr{B}}$, as well. However, in order e.g. to localize fixed points when $\widetilde{\mathscr{A}}=\widetilde{\mathscr{B}}$ in agreement with Theorem 2.1 in[6], we are interested in finding the smallest, rather than the largest, compact set on which the stretching relation is fulfilled. Such need arises also when trying to prove the presence of chaos, in which case the stretching relation in (2.1) has to be satisfied at least with respect to two pairwise disjoint compact sets playing the role of K.[52] Indeed, the result that we will use in Sec. IV and Sec. V reads as follows:

Theorem II.1 *Let $\widetilde{\mathscr{R}}:=(\mathscr{R},\mathscr{R}^-)$ be an oriented rectangle of $\mathbb{R}^2$ and let $F:\mathscr{R}\to\mathbb{R}^2$ be a function. If K_0 and K_1 are disjoint compact subsets of $\mathscr{R}$ such that*

$$(K_i,F):\widetilde{\mathscr{R}}\overset{\sim}{\Rightarrow}\widetilde{\mathscr{R}},\ \textit{for } i=0,1, \tag{2.2}$$

then F induces chaotic dynamics on two symbols on $\mathscr{R}$ relatively to K_0 and K_1, *i.e., setting $K:=K_0\cup K_1$ and introducing the nonempty compact set*

$$Y:=\bigcap_{n=0}^{\infty}F^{-n}(K),$$

there exists a nonempty compact set $X\subseteq Y\subseteq K$, such that:

(*i*) $F(X)=X$;

(*ii*) *$F\restriction_X$ is semiconjugate to the one-sided Bernoulli shift on two symbols σ, that is, there exists a continuous map π from X onto*[53] $\Sigma_2^{\oplus}:=\{0,1\}^{\mathbb{N}}$, *endowed with the distance*

$$\hat{d}(\boldsymbol{s}',\boldsymbol{s}''):=\sum_{i\in\mathbb{N}}\frac{|s_i'-s_i''|}{2^{i+1}},$$

for $\boldsymbol{s}'=(s_i')_{i\in\mathbb{N}}$ and $\boldsymbol{s}''=(s_i'')_{i\in\mathbb{N}}\in\Sigma_2^{\oplus}$, such that $\pi\circ F=\sigma\circ\pi$, where $\sigma:\Sigma_2^{\oplus}\to\Sigma_2^{\oplus}$, $\sigma((s_i)_i):=(s_{i+1})_i$, $\forall i\in\mathbb{N}$;

(*iii*) *the set of the periodic points of $F\restriction_Y$ is dense in X and the preimage $\pi^{-1}(\boldsymbol{s})\subseteq X$ of every k-periodic sequence $\boldsymbol{s}=(s_i)_{i\in\mathbb{N}}\in\Sigma_2^{\oplus}$ contains at least one k-periodic point.*

Furthermore, from conclusion (ii) it follows that:

(*iv*)

$$h_{\mathrm{top}}(F)\geq h_{\mathrm{top}}(F\restriction_X)\geq h_{\mathrm{top}}(\sigma)=\log(2),$$

where h_{top} is the topological entropy (see[54] *for a definition);*

(v) *there exists a compact invariant set $V \subseteq X$ such that $F|_V$ is semiconjugate to the one-sided Bernoulli shift on two symbols, topologically transitive and displays sensitive dependence on initial conditions.*

Proof. The result immediately follows by combining Definition 2.2 in[6] with Theorems 2.2 and 2.3 therein. □

Given Theorem II.1, the SAP method, that allows to prove the presence of chaotic dynamics for a continuous planar map, consists in finding a generalized rectangle inside its domain which, if suitably oriented, contains (at least) two disjoint compact subsets on which the stretching relations in (2.2) are fulfilled. This means that we need to detect a generalized rectangle that is stretched at least twice across itself by the map under analysis, when keeping its orientation unchanged (see Note 49). If we succeed in such task, all the features related to chaos listed in Theorem II.1 will follow for our system. In particular, since for any continuous self-map Φ of a compact topological space it holds that $h_{\text{top}}(\Phi^n) = n\,h_{\text{top}}(\Phi)$ for $n \geq 1$, where $h_{\text{top}}(\Phi)$ denotes the topological entropy of Φ and Φ^n is its n-th iterate (cf. Theorem 2 in[54]), in order to show the existence of chaos for a map, at least in the sense of positive topological entropy, recalling also (iv) in Theorem II.1, it is sufficient to prove that one of its forward iterates is semiconjugate to the Bernoulli shift on two (or more) symbols (see[12]), for instance by applying the SAP technique to that forward iterate.[55] This is the strategy that we will follow in Sec. V, where we shall apply the SAP method to the second iterate of the map G associated with System (3.1), so as to obtain weaker parameter conditions with respect to those, that will be found in Sec. IV, ensuring the emergence of chaotic dynamics when dealing with the first iterate of G. Moreover, we will see that the consideration of G^2 allows to detect attractive chaotic sets, while the numerical simulations we performed do not highlight the presence of chaotic attractors when dealing with G. Namely, in general, as discussed in[6], via Theorem II.1 we only prove the existence of an invariant, chaotic set, not its attractiveness.

We conclude the present discussion with some comments, motivated by what we will show in Sec. IV, about how the SAP method looks like when dealing with 1D maps. Namely, a pair $\widetilde{I} = (I, I^-)$, where $I = [a,b] \subset \mathbb{R}$ is a compact interval and $I^- = \{a,b\}$ is the set of its endpoints, may be seen as a degenerate oriented rectangle. Accordingly, the stretching property $(K,f) : \widetilde{I} \overset{\sim}{\Rightarrow} \widetilde{I}$, with $K \subseteq I$ compact set on which the function $f : I \to \mathbb{R}$ is continuous, is equivalent to the fact that K contains a compact interval I_0 such that $f(I_0) = I$. Hence, in the one-dimensional case, the stretching along the paths relation coincides with the classical covering relation considered e.g. in[56], i.e., in the

1D framework $(K,f):\widetilde{I}\multimap\widetilde{I}$ becomes I f-covers I. Moreover, noticing that, in the just described scenario, we actually have $(I_0,f):\widetilde{I}\multimap\widetilde{I}$, then, if I contains two disjoint compact intervals I_0 and I_1 on which f is continuous and such that $f(I_j)=I$, for $j\in\{0,1\}$, we enter the setting of Theorem II.1, with $\widetilde{I}$ playing the role of $\widetilde{\mathscr{R}}$ and with $K_j=I_j$, so that the conclusions listed therein about the chaotic features of the system hold true in the one-dimensional framework, too. Indeed, according to the results in Sec. 5 in[4], Theorem II.1 holds true when dealing with oriented N-dimensional rectangles for any $N\geq 3$, in addition to the cases $N=1$ and $N=2$.

III. THE MODEL

Following Yousefi et al. in[1], in the next sections we will deal with the discrete-time system

$$\begin{cases} x(t+1)=\mu_1 x(t)(1-x(t))+\gamma_1 y(t) \\ \\ y(t+1)=\mu_2 y(t)(1-y(t))+\gamma_2 x(t) \end{cases} \tag{3.1}$$

composed of two coupled logistic maps, for $\mu_1,\mu_2\in[0,4]$ and $\gamma_1,\gamma_2\in\mathbb{R}$.
We recall that, according to the construction in[1], the model above describes two interdependent economies, characterized by two competitive markets each, with a demand link between them. In particular, the variables x and y, being related to production, cannot be negative. As concerns γ_1 and γ_2, due to their interconnecting role between the two economies, they are called coupling coefficients in[1] and are therein interpreted as trade policy parameters. Because of their different economic meaning, we stress that the linking parameters in[57–60] can take just non-negative values, while in[1] γ_1 and γ_2 can be larger or smaller than 0. If $\gamma_1=\gamma_2=0$, no trade is present, with the two markets being totally disconnected, and the model becomes

$$\begin{cases} x(t+1)=\mu_1 x(t)(1-x(t)) \\ \\ y(t+1)=\mu_2 y(t)(1-y(t)) \end{cases} \tag{3.2}$$

The choice made in[1] of focusing on $\mu_1,\mu_2\in[0,4]$, rather than on larger sets of positive values for μ_1,μ_2, comes from the fact that the 1D logistic map

$$g(x)=\mu x(1-x) \tag{3.3}$$

is a unimodal function taking non-negative values for $x\in[0,1]$ only. Since g has a unique maximum point located in $x=\frac{1}{2}$, with $g(\frac{1}{2})=\frac{\mu}{4}$, the logistic function maps the interval $[0,1]$ into itself

just for $\mu \in [0,4]$, while for $\mu > 4$ the forward iterates of almost all initial points limit to $-\infty$ (cf. Fig. 2 and the explanations in Sec. IV).

Calling $G = (G_1, G_2) : \mathbb{R}^2_+ \to \mathbb{R}^2$ the continuous function associated with System (3.1), whose components are

$$\begin{aligned} G_1(x,y) &:= \mu_1 x(1-x) + \gamma_1 y, \\ G_2(x,y) &:= \mu_2 y(1-y) + \gamma_2 x, \end{aligned} \tag{3.4}$$

where we set $\mathbb{R}^2_+ := \{(x,y) \in \mathbb{R}^2 : x \geq 0, y \geq 0\}$, we are going to show how to apply the Stretching Along the Paths method, whose main features have been recalled in Sec. II, to the first iterate of G in Sec. IV, and to its second iterate in Sec. V.

IV. THE ANALYSIS OF THE FIRST ITERATE

Focusing, in the present section, on the first iterate of the map $G = (G_1, G_2) : \mathbb{R}^2_+ \to \mathbb{R}^2$ in (3.4), we stress that even if, in principle, G_1 and G_2 can be negative, we will restrict our attention on parameter values and subsets of $\mathbb{R}^2_+$ for which G_1 and G_2 are nonnegative, as required by the economic meaning of the variables. Namely, according to Theorem II.1, if the SAP relations in (2.2) are satisfied for G, there exists a nonempty set on which the map is chaotic and, thanks to the parameter conditions that we will impose in the statement of Proposition IV.1, the chaotic invariant set will lie entirely in the first quadrant. In more detail, we are going to investigate for which model parameter values the SAP relations in (2.2) are satisfied for the map G when taking a generalized rectangle in the family $\mathscr{R}$ of (standard) rectangles of the first quadrant, whose elements are given by

$$\mathscr{R} = \mathscr{R}(c) = [0,1] \times [0,c],$$

and when orienting it by setting

$$\mathscr{R}^-_\ell := \{0\} \times [0,c] \quad \text{and} \quad \mathscr{R}^-_r := \{1\} \times [0,c]. \tag{4.1}$$

Such choice for the rectangle is motivated by the simplicity in the computations that are required for the verification of (2.2), when imposing that G produces a folding on $\mathscr{R}$. Moreover, recalling that the 1D logistic map g in (3.3) takes non-negative values just for $x \in [0,1]$, in order to try to have G_1 and G_2 nonnegative on $\mathscr{R}$, we will confine ourselves to $c \in (0,1]$, so that $\mathscr{R} \subseteq [0,1] \times [0,1]$. In particular, we will see in the proof of Proposition IV.1 that some of the parameter conditions which

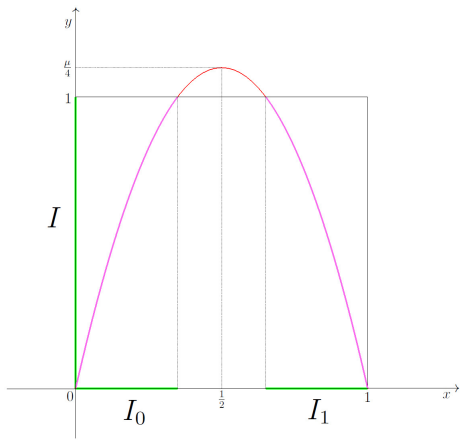

FIG. 2. The graph of g in (3.3) for $\mu > 4$. Since $g(\frac{1}{2}) = \frac{\mu}{4} > 1$, there exist two disjoint compact subintervals I_0 and I_1 of $I = [0,1]$ such that $g(I_j) = I$ for $j \in \{0,1\}$. Notice however that $g(I) \not\subseteq I$.

imply the presence of chaotic dynamics change according to whether $c \in \left(0, \frac{1}{2}\right)$ or $c \in \left[\frac{1}{2}, 1\right]$, as a consequence of the fact that g has a unique maximum point located in $x = \frac{1}{2}$ (cf. (4.3) and (4.4)). Nonetheless, for all $c \in (0,1]$ it happens that the SAP relations in (2.2) are satisfied for the map G just when one parameter between μ_1 (if the expansion occurs along the x-direction, as considered in Proposition IV.1) and μ_2 (if the expansion occurs along the y-direction, cf. Note 63) exceeds 4. We stress that this issue is not related to the choice of the domain on which the SAP method is applied, being instead a consequence of the fact that, as observed in Sec. 3 in[6], it is possible to prove that for g in (3.3) the stretching along the paths relation, which in the 1D framework coincides with the classical covering relation considered e.g. in[56] (cf. the end of Sec. II), is satisfied with respect to two disjoint compact subintervals I_0 and I_1 of $I = [0,1]$ just when $\mu > 4$ (see Fig. 2), so that g does not map the interval $[0,1]$ into itself and almost all orbits starting from I negatively diverge. Such weak point will be fixed in Sec. V, where, dealing with G^2, we will see that the SAP technique can be applied with both μ_1 and μ_2 lying in $[0,4]$, so that, differently from what occurs with G, the chaotic set, whose existence is guaranteed by Theorem II.1, will be attractive, as confirmed by the numerical simulations in Fig. 7 which highlight the existence of a chaotic attractor.

Despite this drawback arising with the application of the SAP method to G, we chose to present the corresponding result in Proposition IV.1 because it allows to understand how the SAP technique works in a simpler setting, which will then be modified, probably becoming less intuitive, when dealing with G^2 in Sec. V. In particular, in Proposition IV.1 we focus on nonnull values for the

coupling coefficients γ_1 and γ_2, since we are interested in understanding the role they play in the emergence on chaotic dynamics.

Proposition IV.1 *For the model parameters satisfying the next conditions*

$$\mu_1 > 4, \quad \mu_2 < 2, \quad \frac{1}{c}\left(1-\frac{\mu_1}{4}\right) < \gamma_1 < 0, \tag{4.2}$$

as well as

$$0 < \gamma_2 \leq c\,(1-\mu_2(1-c)) \tag{4.3}$$

for $c \in (0, \frac{1}{2})$, *or*

$$0 < \gamma_2 \leq c - \frac{\mu_2}{4} \tag{4.4}$$

for $c \in [\frac{1}{2}, 1]$, *the function* G *in* (3.4) *induces chaotic dynamics on two symbols on* $\mathscr{R} = \mathscr{R}(c) = [0,1]\times[0,c]$ *relatively to two suitable disjoint compact subsets* K_0 *and* K_1 *of* $\mathscr{R}$, *and thus all the properties listed in Theorem II.1 are satisfied for* G.

Proof. In order to apply Theorem II.1 to reach the desired conclusions, we have to check that there exist two disjoint compact subsets K_0 and K_1 of $\mathscr{R}$ with respect to which the stretching relations

$$(K_i, G) : \widetilde{\mathscr{R}} \twoheadrightarrow \widetilde{\mathscr{R}} \quad \text{for } i = 0, 1 \tag{4.5}$$

are fulfilled, where we recall that $\widetilde{\mathscr{R}} := (\mathscr{R}, \mathscr{R}^-)$, with $\mathscr{R}^- := \mathscr{R}_\ell^- \cup \mathscr{R}_r^-$, and $\mathscr{R}_\ell^-$ and $\mathscr{R}_r^-$ as introduced in (4.1).

We split our proof into two main steps.

Step 1: Firstly, we show that the conditions in (4.2) guarantee the validity of the following properties for G_1

$$G_1(0,y) \leq 0, \;\; G_1(1,y) \leq 0, \;\; G_1\left(\frac{1}{2}, y\right) > 1, \forall y \in [0,c], \tag{4.6}$$

according to which a stretching and a folding[61] along the x-direction occurs, and we prove that, depending on the value of c, the conditions in (4.3) or in (4.4) imply the next features for G_2

$$\min_{(x,y)\in\mathscr{R}} G_2(x,y) \geq 0, \quad \max_{(x,y)\in\mathscr{R}} G_2(x,y) \leq c, \tag{4.7}$$

that describe a compression[62] along the y-direction.[63]

Step 2: As a second and final stage in the process, we will verify that, under (4.6) and (4.7), the SAP relations in (4.5) are fulfilled relatively to two suitably defined disjoint compact subsets K_0 and K_1 of $\mathscr{R}$ (cf. (4.8)).

In regard to Step 1, as concerns (4.6) we notice that, for every $y \in [0,c]$, we have $G_1(0,y) = G_1(1,y) = \gamma_1 y$ which is non-positive for $\gamma_1 \leq 0$. Discarding null values for the coupling coefficients γ_1 and γ_2, we then obtain $\gamma_1 < 0$ as sufficient condition for $G_1(0,y) \leq 0$ and $G_1(1,y) \leq 0$. With a negative value for γ_1, for $y \in [0,c]$ it holds that $G_1\left(\frac{1}{2},y\right) = \frac{\mu_1}{4} + \gamma_1 y \geq \frac{\mu_1}{4} + \gamma_1 c$, that is larger than 1 for $0 > \gamma_1 > \frac{1}{c}\left(1 - \frac{\mu_1}{4}\right)$, which is possible just with $\mu_1 > 4$. Hence, the first and the third conditions in (4.2) imply (4.6). Turning now to (4.7), we start by noticing that G_2 admits a minimum and a maximum value on $\mathscr{R}$ due to Weierstrass Theorem. Since the gradient of G_2 never vanishes when γ_2 is nonnull, by Fermat Theorem the minimum and maximum points of G_2 need to belong to the boundary of $\mathscr{R}$. In particular, $G_2(x,0) = \gamma_2 x$ is non-negative for $\gamma_2 > 0$ and in such case we also have $0 \leq G_2(x,c) = \mu_2 c(1-c) + \gamma_2 x \leq \mu_2 c(1-c) + \gamma_2$, recalling that $x \in [0,1]$. Moreover, for $y \in [0,c]$, if $c \in (0,\frac{1}{2})$, then $0 \leq G_2(0,y) = \mu_2 y(1-y) \leq \mu_2 c(1-c)$ and $0 \leq G_2(1,y) = \mu_2 y(1-y) + \gamma_2 \leq \mu_2 c(1-c) + \gamma_2$, while, if $c \in [\frac{1}{2},1]$, then $0 \leq G_2(0,y) \leq \frac{\mu_2}{4}$ and $0 \leq G_2(1,y) \leq \frac{\mu_2}{4} + \gamma_2$. Hence, for $c \in (0,\frac{1}{2})$ it holds that $\min_{(x,y)\in\mathscr{R}} G_2(x,y) \geq 0$ and $\max_{(x,y)\in\mathscr{R}} G_2(x,y) = \mu_2 c(1-c) + \gamma_2$, so that (4.7) is implied by (4.3). If instead $c \in [\frac{1}{2},1]$ we have $\min_{(x,y)\in\mathscr{R}} G_2(x,y) \geq 0$ and $\max_{(x,y)\in\mathscr{R}} G_2(x,y) = \frac{\mu_2}{4} + \gamma_2$, so that (4.7) is implied by (4.4). This concludes the first half of the proof.

As concerns the second half of it, in order to check that under (4.6) and (4.7) the SAP relations in (4.5) are fulfilled, we set

$$\mathscr{R}_0 := \left[0,\frac{1}{2}\right] \times [0,c], \quad \mathscr{R}_1 := \left[\frac{1}{2},1\right] \times [0,c]$$

and define

$$K_0 := \mathscr{R}_0 \cap G^{-1}(\mathscr{R}), \quad K_1 := \mathscr{R}_1 \cap G^{-1}(\mathscr{R}). \tag{4.8}$$

Notice that K_0 and K_1 are compact subsets of $\mathscr{R}$ because they are closed subsets of the compact sets $\mathscr{R}_0$ and $\mathscr{R}_1$, respectively. Furthermore, K_0 and K_1 are disjoint because they could intersect just along the vertical segment $S := \left\{\frac{1}{2}\right\} \times [0,c]$, but, by the third condition in (4.6), S is mapped by G outside $\mathscr{R}$. We also remark that G is continuous on K_0 and on K_1, since it is continuous on $\mathbb{R}^2_+$. Moreover, let us take a generic path $\gamma : [0,1] \to \mathscr{R}$ with $\gamma(0)$ and $\gamma(1)$ belonging to the different components of $\mathscr{R}^-$. Then, by (4.6) and (4.7), as well as by the definition of K_0 and K_1 in (4.8), there exist two disjoint subintervals $[t_0', t_0''], [t_1', t_1''] \subseteq [0,1]$ such that $\gamma([t_i', t_i'']) \subseteq K_i$ and $G(\gamma([t_i', t_i''])) \subseteq \mathscr{R}$ for $i \in \{0,1\}$, with $G(\gamma(t_i'))$ and $G(\gamma(t_i''))$ belonging to the different components of $\mathscr{R}^-$. Recalling Definition II.1, the proof of (4.5), and thus of our result, is complete. □

We remark that the parameter conditions in (4.3) (valid for $c \in \left(0, \frac{1}{2}\right)$) and in (4.4) (valid for $c \in \left[\frac{1}{2}, 1\right]$) coincide for $c = \frac{1}{2}$ and that, in such case, together with (4.2), they read as

$$\mu_1 > 4, \quad \mu_2 < 2, \quad 2\left(1 - \frac{\mu_1}{4}\right) < \gamma_1 < 0, \quad 0 < \gamma_2 \leq \frac{1}{2} - \frac{\mu_2}{4}. \tag{4.9}$$

Looking at (4.2) and (4.4), we also notice that the set of values for γ_2 for which there is chaos according to Proposition IV.1 is larger when c is close to 1, but the set of admissible values for γ_1, due to its negativity, shrinks with an increase in c. In view of mediating between such two opposite tendencies, we will consider $c = \frac{1}{2}$ in Fig. 3, where for $\mu_1 = 4.5$, $\mu_2 = 1.5$, $\gamma_1 = -0.2$ and $\gamma_2 = 0.1$ we illustrate in (a) how the rectangle $\mathscr{R} = \mathscr{R}\left(\frac{1}{2}\right)$ is transformed by G and in (b) we show the compact sets K_0 and K_1, defined as in (4.8), for which the stretching relations in (4.5) hold true. Notice that for the chosen parameter values the conditions in (4.9) are indeed satisfied.

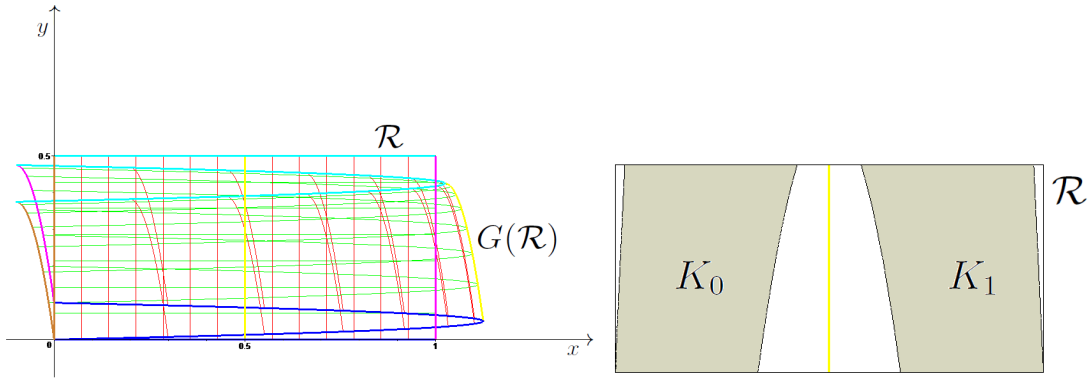

(a) (b)

FIG. 3. For $\mu_1 = 4.5$, $\mu_2 = 1.5$, $\gamma_1 = -0.2$ and $\gamma_2 = 0.1$, we show in (a) that G in (3.4) stretches along the x-direction and folds $\mathscr{R} = [0,1] \times \left[0, \frac{1}{2}\right]$ so that $G(\mathscr{R})$ intersects $\mathscr{R}$ twice, in such a way that the stretching relations in (4.5) are fulfilled with K_0 and K_1 defined as in (4.8) and depicted in (b), when $\mathscr{R}$ is oriented as in (4.1). Notice that, by construction, K_0 and K_1 are separated by the vertical segment $S := \left\{\frac{1}{2}\right\} \times \left[0, \frac{1}{2}\right]$ (in yellow), which is mapped by G outside $\mathscr{R}$. In (a) we used the same color to draw a line segment and its image through G. Moreover, in order to better illustrate how $G(\mathscr{R})$ is obtained starting from $\mathscr{R}$, we showed in (a) how G acts on a grid covering $\mathscr{R}$.

We conclude the present section about the analysis of G in (3.4) by stressing that, similar to what happens when applying the SAP method to the first iterate of the map associated with the 2D System (3.1), in which, as discussed before Proposition IV.1, one parameter between μ_1 and μ_2 has to be larger than 4, also with a 3D formulation of G the same issue arises, and thus the chaotic

set, whose existence is guaranteed by the three-dimensional counterpart of Theorem II.1,[64] is not attractive, since almost all the trajectories diverge.

Indeed, abstracting from its economic interpretation given in[1], the simplest way to extend (3.4) to a 3D framework probably consists in dealing with the continuous function $\widehat{G} = (\widehat{G}_1, \widehat{G}_2, \widehat{G}_3) : \mathbb{R}^3_+ \to \mathbb{R}^3$, whose components are[65]

$$\begin{aligned} \widehat{G}_1(x,y,z) &:= \mu_1 x(1-x) + \gamma_{11} y + \gamma_{12} z, \\ \widehat{G}_2(x,y,z) &:= \mu_2 y(1-y) + \gamma_{21} x + \gamma_{22} z, \\ \widehat{G}_3(x,y,z) &:= \mu_3 z(1-z) + \gamma_{31} x + \gamma_{32} y, \end{aligned} \tag{4.10}$$

where $\mathbb{R}^3_+ := \{(x,y,z) \in \mathbb{R}^3 : x \geq 0, y \geq 0, z \geq 0\}$ is the first octant of $\mathbb{R}^3$.

In order to verify that the 3D version of the stretching relations[66] in (4.5) for $\widehat{G}$, we need to assume that two out of the x-, y- and z-directions are compressive, and that the remaining one is expansive. Just the expansion along one direction, whatever it is, requires the corresponding value for the μ_i parameter, $i \in \{1,2,3\}$, to exceed 4. In fact, the analysis performed above and the kind of findings obtained in the present section would be valid also when studying System (4.10). In more detail, its investigation would follow similar lines to[7,8], where the SAP method has been applied to 3D discrete-time settings. However, in order not to overburden the paper, we prefer to focus on the 2D framework only. One more aspect supporting our choice lies in the fact that the described weak point connected with the application of the SAP method to the dynamical system generated by $\widehat{G}$ could be fixed by dealing with its second iterate, similar to what we shall do in the 2D framework in Sec. V, where we will consider G^2, with G as in (3.4). Since working with the second iterate of $\widehat{G}$ would lead to cumbersome computations, in the next section we will confine ourselves to the study of the two-dimensional setting, just showing some illustrations of the 3D framework in Figs. 8 and 9.

V. DEALING WITH THE SECOND ITERATE

In view of trying to find more general conditions on the model parameters than those derived in Proposition IV.1 but still guaranteeing the emergence of chaotic dynamics, in the present section we apply the SAP method to the second iterate of G in (3.4).

As an intermediate step in order to explain how this can be performed, we start by focusing on

the case in which the two economies are totally disconnected, so that we consider (3.2) in place of (3.1) and we are thus led to deal with the logistic map $g(x)$ in (3.3), together with its second iterate. Using then a pertubative method, grounded on what learned in the 1D framework and in which the value of the linking parameters is gradually increased, we will be able to exploit a similar geometry also in the two-dimensional framework.[67]

We have seen in Fig. 2 the way the 1D version of the SAP method, described at the end of Sec. II, can be applied to g on the interval $[0,1]$, in which case its maximum value has to exceed 1, condition requiring $\mu > 4$. However, in such manner the forward iterates of almost all initial points limit to $-\infty$. On the other hand, as observed in Sec. 3 in[6] (cf. Fig. 2 therein), when dealing with the second iterate of g it is possible to apply the SAP method on a subset of $[0,1]$ for $\mu < 4$, as well. We analyze more closely the needed geometry with the aid of Fig. 4, in which we show two disjoint compact subintervals[68] J_L and J_R of $[0,1]$ such that $g^2(J_i) := J \supset J_L \cup J_R$ for $i \in \{L,R\}$. Thanks to this construction, the one-dimensional version of the stretching conditions in (2.2) is satisfied for g^2 and all the features related to chaos listed in Theorem II.1 are fulfilled for the second iterate of g. In particular, from (iv) in Theorem II.1 it holds that $h_{\text{top}}(g^2) \geq \log(2)$, where in general $h_{\text{top}}(\Phi)$ denotes the topological entropy of Φ for any continuous self-function[69] Φ of a compact topological space Z. Then, since $h_{\text{top}}(g^2) = 2h_{\text{top}}(g)$ by Theorem 2 in[54], it follows that $h_{\text{top}}(g) \geq \log(\sqrt{2})$ and thus the topological entropy of g is positive. We recall that the positivity of the topological entropy for a map is generally considered as one of the trademarks of chaos for the associated dynamical system.

In view of exploiting a construction similar to that in Fig. 4 also in the 2D framework, we need to look better at how the subintervals J_L and J_R of $[0,1]$ are obtained in that picture. To such aim, we notice that the expression for the second iterate of the logistic map reads as

$$g^2(x) = \mu^2 x(1-x)(1-\mu x+\mu x^2), \tag{5.1}$$

and it is then a function vanishing for $x = 0$ and $x = 1$, whose graph on the interval $[0,1]$ is symmetric with respect to $x = \frac{1}{2}$, since a direct check shows that $g^2(\frac{1}{2}-\alpha) = g^2(\frac{1}{2}+\alpha)$, for every $\alpha \in [0,\frac{1}{2}]$. Moreover, studying its derivative, we find that g^2 admits $x_{M_L} := \frac{1}{2} - \frac{1}{2}\sqrt{1-\frac{2}{\mu}}$, $x = \frac{1}{2}$ and $x_{M_R} := \frac{1}{2} + \frac{1}{2}\sqrt{1-\frac{2}{\mu}}$ as critical points. Since x_{M_L} and x_{M_R} are well-defined and not coinciding just for $\mu > 2$, it holds that g^2 for $\mu \leq 2$ is a unimodal function with a maximum point in $x = \frac{1}{2}$, looking then similar to g in Fig. 2, while, for $\mu > 2$, g^2 has a minimum point in $x = \frac{1}{2}$, and two symmetric maximum points in $x = x_{M_L}$ and $x = x_{M_R}$. In particular, it holds that

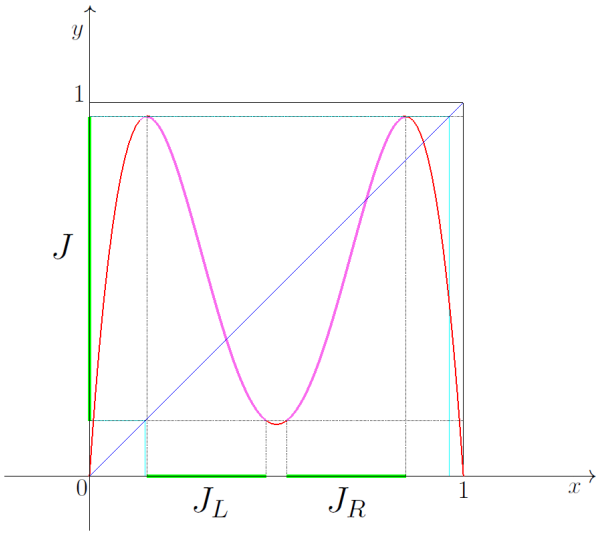

FIG. 4. The graph of g^2 in (5.1) for $\mu^* < \mu < 4$ and $\varepsilon_d > 0$ small enough, so that the compact disjoint subintervals $J_L := [x_{M_L}, x_{m_L}]$ and $J_R := [x_{m_R}, x_{M_R}]$ of $J := [m+\varepsilon_d, M] \subset [0,1]$ satisfy the condition $g^2(J_i) = J$ for $i \in \{L, R\}$.

$m := g^2(\frac{1}{2}) = \frac{\mu^2}{4}\left(1 - \frac{\mu}{4}\right) > 0$ and $M := g^2(x_{M_L}) = g^2(x_{M_R}) = \frac{\mu}{4} < 1$ for $\mu < 4$. Turning back to Fig. 4, we notice that for $\mu < 4$, in order for J_L and J_R to be disjoint, we can choose the right endpoint of J_L and the left endpoint of J_R to be the solutions, that we will call x_{m_L} and x_{m_R}, closest to $x = \frac{1}{2}$ to the equation $g^2(x) = m + \varepsilon_d$, with ε_d a small, positive quantity. The left endpoint of J_L and the right endpoint of J_R will instead coincide with x_{M_L} and x_{M_R}, respectively, i.e., $J_L := [x_{M_L}, x_{m_L}]$ and $J_R := [x_{m_R}, x_{M_R}]$, so that $g^2(J_i) := J = [m+\varepsilon_d, M]$, for $i \in \{L, R\}$. As mentioned above, in order to have the one-dimensional version of (2.2) satisfied for g^2, so that all the properties listed in Theorem II.1 are fulfilled, we need that J contains both J_L and J_R. Let us then investigate for which parameter values (maintaining that $\varepsilon_d > 0$ is small enough) the analytical conditions guaranteeing that $J \supset J_L \cup J_R$, i.e., $m + \varepsilon_d < x_{M_L}$ and $x_{M_R} < M$, are fulfilled. Direct computations allow to conclude that when $\varepsilon_d = 0$ both conditions are satisfied for $\mu > \mu^* := 3.83188$. Hence, by continuity, if $\varepsilon_d > 0$ is sufficiently small, the conditions above hold true for large enough values of μ, which however can be less than 4. Indeed, in Fig. 4 we considered $\mu = 3.85$ and $\varepsilon_d = 0.1$, so that $J_L = [x_{M_L}, x_{m_L}] = [0.1534, 0.4730]$ and $J_R = [x_{m_R}, x_{M_R}] = [0.5270, 0.8466]$ are both contained in $J = [m+\varepsilon_d, M] = [0.1490, 0.9625]$.

In order to try to exploit a similar construction in the 2D framework with the second iterate of G

in (3.4), let us at first notice that it can be written as $G^2 = (G_1^2, G_1^2)$, with

$$G_1^2(x,y) := g_{\mu_1}^2(x) + \gamma_1 \left[\mu_1 y(1-\gamma_1 y - 2\mu_1 x(1-x)) + \mu_2 y(1-y) + \gamma_2 x\right],$$

$$G_2^2(x,y) := g_{\mu_2}^2(y) + \gamma_2 \left[\mu_2 x(1-\gamma_2 x - 2\mu_2 y(1-y)) + \mu_1 x(1-x) + \gamma_1 y\right],$$

where, recalling (5.1), we set $g_{\mu_i}^2(z) := \mu_i^2 z(1-z)(1-\mu_i z+\mu_i z^2)$ with $(i,z) \in \{(1,x),(2,y)\}$. This means that, assuming that γ_1 and γ_2 are small in absolute value, we can see $G_1^2(x,y)$ and $G_2^2(x,y)$ as perturbations of $g_{\mu_1}^2(x)$ and $g_{\mu_2}^2(y)$, respectively, and thus we can transfer to G^2 what we observed about the second iterate of the logistic map.

In particular, in view of obtaining that a suitable generalized rectangle is transformed by G^2 so that a stretching and a folding occurs along e.g. the x-direction, while a compression is produced along the y-direction, we will assume that $\mu_1 > 3.83188$, so that for G_1^2 a geometrical configuration similar to that in Fig. 4, though two-dimensional, emerges, while it is more convenient to suppose that μ_2 is lower than 2, so that computations are simplified by the fact that $g_{\mu_2}^2(y)$ is unimodal. In regard to the choice of the generalized rectangle $\mathscr{Q}$, due to the presence of the coupling coefficients γ_1 and γ_2 and of their perturbing effect with respect to the 1D framework, rather than considering the square $J_1 \times J_1$, with $J_1 = [m_1 + \varepsilon_d, M_1]$ where we set $m_1 := \frac{\mu_1^2}{4}\left(1 - \frac{\mu_1}{4}\right)$, $M_1 := \frac{\mu_1}{4}$ and ε_d is a small positive quantity, we will deal with the square $\bar{J}_1 \times \bar{J}_1$, with $\bar{J}_1 := [m_1 + \varepsilon_d, M_1 - \varepsilon_u]$ where $\varepsilon_u > 0$ introduces a little distance for the right endpoint of $\bar{J}_1$ from the maximum value of $g_{\mu_1}^2(x)$. As we shall see below, this precaution, together with suitable conditions which may vary according to the considered parameter configuration (cf. (5.5), (5.6) and (5.7)), allow for a double crossing, from left to right, between $G^2(\mathscr{Q})$ and $\mathscr{Q} := \bar{J}_1 \times \bar{J}_1$, when suitably choosing $\varepsilon_d > 0$ and $\varepsilon_u > 0$, and on orienting $\mathscr{Q}$ by setting

$$\mathscr{Q}_\ell^- := \{M_1 - \varepsilon_u\} \times [m_1 + \varepsilon_d, M_1 - \varepsilon_u], \quad \mathscr{Q}_r^- := \{m_1 + \varepsilon_d\} \times [m_1 + \varepsilon_d, M_1 - \varepsilon_u] \tag{5.2}$$

so as to obtain the oriented rectangle $\widetilde{\mathscr{Q}} := (\mathscr{Q}, \mathscr{Q}^-)$, with $\mathscr{Q}^- := \mathscr{Q}_\ell^- \cup \mathscr{Q}_r^-$. The need of defining as left/right sides of $\mathscr{Q}$ what are usually called the right/left sides of the square comes from the fact that G_1^2, when it is expansive, produces a stretching along the x-direction whose orientation is reversed with respect to that produced by G_1, as it is evident comparing Fig. 3 with Figs. 5 and 6. Such difference is reflected by the conditions in (5.5) and (5.7), that replace (4.6). However, as stressed in Sec. II, those left/right names for the sides of an oriented rectangle are not binding from a geometric viewpoint, being purely conventional. We also remark that, in view of minimizing the differences with respect to the proof of Proposition IV.1, we shall define below $\mathscr{Q}_0$ and $\mathscr{Q}_1$, as well

as H_0 and H_1 in (5.4), similar to (4.8), without inverting them, since there is not a fixed ordering to be assigned to the compact sets on which the stretching relations are satisfied.

To try to reach our conclusions about G^2, let us observe the structure of the proof of Proposition IV.1, that will essentially remain unchanged when dealing with the second iterate of G, even if in the latter case we will have to focus on some specific parameter configurations. Indeed, it is analytically unfeasible to take into account all the possibilities concerning the sign of the various factors that emerge in the expressions for G_1^2 and G_2^2, when imposing some conditions that those components have to satisfy. Moreover, the conditions needed to apply the SAP method partially change with the considered parameter values. The strategy to prove the presence of chaos for G^2 is still that of applying Theorem II.1, which requires that there exist two disjoint compact subsets H_0 and H_1 of $\mathscr{Q}$ with respect to which the stretching relations

$$(H_i, G^2) : \widetilde{\mathscr{Q}} \twoheadrightarrow \widetilde{\mathscr{Q}} \quad \text{for } i = 0, 1 \tag{5.3}$$

are fulfilled. The kind of arguments employed in Step 2 of the proof of Proposition IV.1 can be applied in the present context, too, and mainly require to adjust notation, when defining

$$\mathscr{Q}_0 := \left[m_1 + \varepsilon_d, \frac{1}{2}\right] \times [m_1 + \varepsilon_d, M_1 - \varepsilon_u], \quad \mathscr{Q}_1 := \left[\frac{1}{2}, M_1 - \varepsilon_u\right] \times [m_1 + \varepsilon_d, M_1 - \varepsilon_u]$$

and

$$H_0 := \mathscr{Q}_0 \cap \left(G^2\right)^{-1}(\mathscr{Q}), \quad H_1 := \mathscr{Q}_1 \cap \left(G^2\right)^{-1}(\mathscr{Q}), \tag{5.4}$$

after having imposed conditions on G_1^2 and G_2^2 bearing some resemblance to (4.6) and (4.7), but adapted to the features of G^2, and being also parameter dependent to a certain degree. As concerns Step 1, rather than providing, like it was in the proof of Proposition IV.1, parameter conditions which guarantee that the components of the map satisfy suitable properties, we focus on two parameter configurations that mainly differ in the sign of γ_1, and we investigate how G_1^2 and G_2^2 have to behave in order to have (5.3) fulfilled for $\widetilde{\mathscr{Q}}$, with ε_d and ε_u fixed in advance. In more detail, for both parameter configurations, we will first deal with the case $\gamma_1 = \gamma_2 = 0$, so that the two economies are isolated, and we then impose conditions on G_1^2 and G_2^2 that ensure the validity of the SAP relations in (5.3) when focusing on sufficiently small (positive or negative) values of γ_1 and γ_2, by exploiting the continuity of G_1^2 and G_2^2.

Analysis with the first parameter configuration

The first parameter set we consider is given by $\mu_1 = 3.96$, $\mu_2 = 2$, $\gamma_1 = -0.025$, $\gamma_2 = 0.16$. As shown in Fig. 5, the SAP technique can be applied to $\mathscr{Q} := \bar{J}_1 \times \bar{J}_1$ when choosing $\varepsilon_d = 0.085$

and $\varepsilon_u = 0.12$, so that $\mathscr{Q} = [0.124, 0.870] \times [0.124, 0.870]$. Let us try to understand why it is so, disregarding for the moment the values of γ_1 and γ_2, that can be assumed to be equal to 0, so that we are in the isolated economy scenario. Focusing at first on the expansive direction, i.e., the horizontal one, we notice that, since $\mu_1 > 2$, then $g^2_{\mu_1}(x)$ has a minimum point in $x = \frac{1}{2}$ and two maximum points in x_{M_L}, x_{M_R} that, in agreement with the construction in Fig. 4, are internal to $\bar{J}_1 = [m_1 + \varepsilon_d, M_1 - \varepsilon_u]$, since it holds that $m_1 + \varepsilon_d = 0.124 < x_{M_L} = 0.148 < x_{M_R} = 0.852 < M_1 - \varepsilon_u = 0.870$. In order to observe an expansion and a folding for G^2 along the x-direction when the two economies are isolated,[70] we could impose $g^2_{\mu_1}(\frac{1}{2}) < m_1 + \varepsilon_d$ and $g^2_{\mu_1}(x_{M_L}) = g^2_{\mu_1}(x_{M_R}) > M_1 - \varepsilon_u$. However, due to the closeness of the maximum points of $g^2_{\mu_1}$ to the endpoints of $\bar{J}_1$, rather than the latter condition, for simplicity's sake we will consider the stronger $g^2_{\mu_1}(m_1 + \varepsilon_d) > M_1 - \varepsilon_u$, which also implies that $g^2_{\mu_1}(M_1 - \varepsilon_u) > M_1 - \varepsilon_u$, recalling that $g^2_{\mu}(x)$ is symmetric with respect to $x = \frac{1}{2}$ for any $\mu > 0$ and observing that $x_{M_L} - (m_1 + \varepsilon_d) = 0.024 > M_1 - \varepsilon_u - x_{M_R} = 0.018$.

Assuming that γ_1 and γ_2 are small in absolute value but nonnull[71], in place of (4.6) we impose

$$G^2_1\left(\frac{1}{2}, y\right) < m_1 + \varepsilon_d, \quad G^2_1(m_1 + \varepsilon_d, y) \geq M_1 - \varepsilon_u, \quad \forall y \in \bar{J}_1, \tag{5.5}$$

meaning that, employing a notation analogous to that used in the proof of Proposition IV.1, the vertical segment $S := \left\{\frac{1}{2}\right\} \times [m_1 + \varepsilon_d, M_1 - \varepsilon_u]$ (depicted in yellow in Fig. 5 (b)) is mapped by G^2_1 on the left of $\mathscr{Q}$, while, recalling the definitions in (5.2), we require that $\mathscr{Q}^-_r$ (depicted in brown in Fig. 5 (b)), and thus $\mathscr{Q}^-_\ell$ (depicted in red in Fig. 5 (b)), are mapped by G^2_1 on the right of $\mathscr{Q}$.

In particular, focusing on the case $\gamma_1 = -0.025$ and $\gamma_2 = 0.16$, as concerns the first condition in (5.5) we have that $G^2_1(\frac{1}{2}, y)$ is increasing for $y \in \bar{J}_1$, since $\frac{d}{dy} G^2_1(\frac{1}{2}, y) = \gamma_1 \big(\mu_1(1 - \frac{\mu_1}{2} - 2\gamma_1 y) + \mu_2 (1 - 2y)\big)$ is positive for $y > \frac{\mu_1(1-\frac{\mu_1}{2})+\mu_2}{2(\gamma_1\mu_1+\mu_2)} = -0.495$, since in the considered scenario γ_1 is negative. Hence, $G^2_1(\frac{1}{2}, y) < m_1 + \varepsilon_d$ on $\bar{J}_1$ is equivalent to $G^2_1(\frac{1}{2}, M_1 - \varepsilon_u) < m_1 + \varepsilon_d$. In regard to $G^2_1(m_1 + \varepsilon_d, y) \geq M_1 - \varepsilon_u$ on $\bar{J}_1$, studying the sign of $\frac{d}{dy} G^2_1(m_1 + \varepsilon_d, y)$, we obtain a minimum point in $y = y_m := \frac{\mu_1(1-2\mu_1(m_1+\varepsilon_d)(1-m_1-\varepsilon_d))+\mu_2}{2(\gamma_1\mu_1+\mu_2)} = 0.670$. Thus, the second condition in (5.5) is equivalent to $G^2_1(m_1 + \varepsilon_d, y_m) \geq M_1 - \varepsilon_u$. Notice that both the derived conditions are satisfied in our framework, since $G^2_1\left(\frac{1}{2}, M_1 - \varepsilon_u\right) = 0.114 < m_1 + \varepsilon_d = 0.124$ and $G^2_1(m_1 + \varepsilon_d, y_m) = 0.949 > M_1 - \varepsilon_u = 0.870$.

Turning now to the compressive direction, i.e., the vertical one, we remark that, assuming for the moment $\gamma_1 = \gamma_2 = 0$, since $\mu_2 = 2$, then $g^2_{\mu_2}(y)$ is a unimodal map, with a maximum point in $y = \frac{1}{2}$ and two minimum points in the endpoints of $\bar{J}_1$. More precisely, since $\frac{1}{2} - m_1 - \varepsilon_d = 0.376 > M_1 - \varepsilon_u - \frac{1}{2} = 0.370$ and thus, recalling that $g^2_{\mu_2}(y)$ is symmetric with respect to $y = \frac{1}{2}$, we have $g^2_{\mu_2}(m_1 + \varepsilon_d) < g^2_{\mu_2}(M_1 - \varepsilon_u)$, to witness a contraction for G^2 along the y-direction when the two

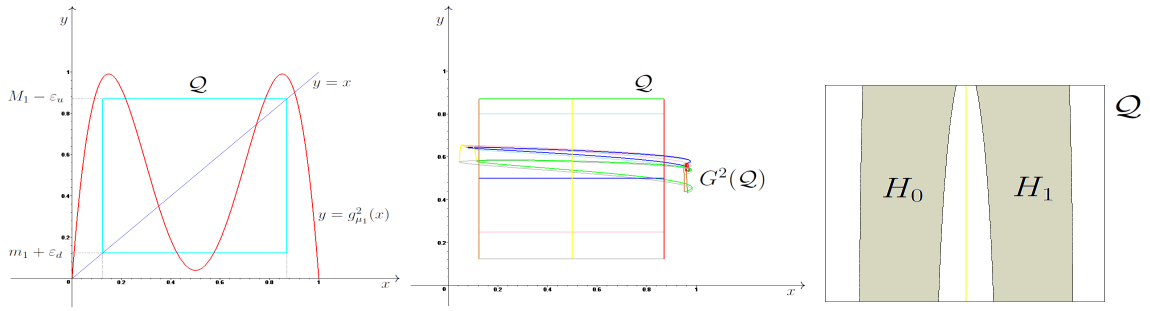

(a) (b) (c)

FIG. 5. For $\mu_1 = 3.96$, $\mu_2 = 2$, $\gamma_1 = -0.025$ and $\gamma_2 = 0.16$, we show in (b) that, for G in (3.4) and for the square $\mathscr{Q} := \bar{J}_1 \times \bar{J}_1 = [0.124, 0.870] \times [0.124, 0.870]$ depicted in (a) it holds that $G^2(\mathscr{Q})$ intersects $\mathscr{Q}$ twice in such a way that the stretching relations in (5.3) are fulfilled for G^2 with H_0 and H_1 defined as in (5.4) and drawn in (c), when $\mathscr{Q}$ is oriented as in (5.2). In (b) we used the same color to draw suitable line segments and their image through G^2.

economies are isolated, we impose, in addition to $g^2_{\mu_2}(\frac{1}{2}) < M_1 - \varepsilon_u$, also $g^2_{\mu_2}(m_1 + \varepsilon_d) > m_1 + \varepsilon_d$, which implies $g^2_{\mu_2}(M_1 - \varepsilon_u) > m_1 + \varepsilon_d$.

Assuming that γ_1 and γ_2 are small in absolute value but nonnull, in place of (4.7) we set

$$G_2^2(x, m_1 + \varepsilon_d) \geq m_1 + \varepsilon_d, \quad G_2^2\left(x, \frac{1}{2}\right) \leq M_1 - \varepsilon_u, \quad \forall x \in \bar{J}_1, \tag{5.6}$$

so that $G_2^2(\mathscr{Q})$ is contained in the infinite horizontal strip $\mathbb{R} \times [m_1 + \varepsilon_d, M_1 - \varepsilon_u]$, that contains $\mathscr{Q}$ as well. Recalling that $\gamma_1 = -0.025$ and $\gamma_2 = 0.16$ in the considered parameter set, since $\frac{d}{dx}G_2^2(x, m_1 + \varepsilon_d) = \gamma_2\big(\mu_2(1 - 2\mu_2(m_1 + \varepsilon_d)(1 - m_1 - \varepsilon_d) - 2\gamma_2 x) + \mu_1(1 - 2x)\big)$, then $G_2^2(x, m_1 + \varepsilon_d)$ has a maximum point in $x = \frac{\mu_2(1 - 2\mu_2(m_1 + \varepsilon_d)(1 - m_1 - \varepsilon_d)) + \mu_1}{2(\mu_1 + \gamma_2\mu_2)} = 0.595$, while the minimum points are located in the endpoints of $\bar{J}_1$. In particular, since $G_2^2(m_1 + \varepsilon_d, m_1 + \varepsilon_d) = 0.431 < G_2^2(M_1 - \varepsilon_u, m_1 + \varepsilon_d) = 0.530$, it holds that the condition $G_2^2(x, m_1 + \varepsilon_d) \geq m_1 + \varepsilon_d$ on $\bar{J}_1$ is equivalent to $G_2^2(m_1 + \varepsilon_d, m_1 + \varepsilon_d) \geq m_1 + \varepsilon_d$. In regard to $G_2^2\left(x, \frac{1}{2}\right) \leq M_1 - \varepsilon_u$ for every $x \in \bar{J}_1$, a study of the sign of $\frac{d}{dx}G_2^2\left(x, \frac{1}{2}\right)$ shows that $G_2^2\left(x, \frac{1}{2}\right)$ has a maximum point in $x = x_M := \frac{\mu_2(1 - \frac{\mu_2}{2}) + \mu_1}{2(\mu_1 + \gamma_2\mu_2)} = 0.463$. Hence, the second inequality in (5.6) is equivalent to $G_2^2\left(x_M, \frac{1}{2}\right) \leq M_1 - \varepsilon_u$. The obtained conditions are satisfied in the considered framework, since $G_2^2(m_1 + \varepsilon_d, m_1 + \varepsilon_d) = 0.431 > m_1 + \varepsilon_d = 0.124$ and $G_2^2\left(x_M, \frac{1}{2}\right) = 0.645 < M_1 - \varepsilon_u = 0.870$.

Analysis with the second parameter configuration

Turning now to the second parameter set,[72] i.e., $\mu_1 = 3.832$, $\mu_2 = 1.7$, $\gamma_1 = 0.1$, $\gamma_2 = 0.2$, the SAP method can be applied to $\mathscr{Q} := \bar{J}_1 \times \bar{J}_1$ when choosing $\varepsilon_d = 0.02$ and $\varepsilon_u = 0.17$, so that

$\mathscr{Q} = [0.174, 0.788] \times [0.174, 0.788]$, as illustrated in Fig. 6. Indeed assuming for the moment that we are in the isolated economy scenario, i.e., that $\gamma_1 = \gamma_2 = 0$, let us start by focusing on the horizontal, expansive direction. Since μ_1 is larger than 2, then $g^2_{\mu_1}(x)$ has a minimum point in $x = \frac{1}{2}$ and two maximum points in x_{M_L}, x_{M_R}, that this time are however external to $\bar{J}_1 = [m_1 + \varepsilon_d, M_1 - \varepsilon_u]$, since it holds that $x_{M_L} = 0.154 < m_1 + \varepsilon_d = 0.174 < M_1 - \varepsilon_u = 0.788 < x_{M_R} = 0.846$. Despite such difference with the construction in Fig. 4, caused by a larger value for ε_u with respect to the first parameter set, as shown in Fig. 6 (a) a double covering of $\bar{J}_1$ is produced by $g^2_{\mu_1}$ when $g^2_{\mu_1}(\frac{1}{2}) < m_1 + \varepsilon_d$ and $g^2_{\mu_1}(M_1 - \varepsilon_u) > M_1 - \varepsilon_u$, since the latter condition also implies that $g^2_{\mu_1}(m_1 + \varepsilon_d) > M_1 - \varepsilon_u$, due to the symmetry of $g^2_{\mu}(x)$ with respect to $x = \frac{1}{2}$ for any $\mu > 0$ and observing that $\frac{1}{2} - (m_1 + \varepsilon_d) = 0.326 > M_1 - \varepsilon_u - \frac{1}{2} = 0.288$. The conditions $g^2_{\mu_1}(\frac{1}{2}) < m_1 + \varepsilon_d$ and $g^2_{\mu_1}(M_1 - \varepsilon_u) > M_1 - \varepsilon_u$ then generate an expansion for G^2 along the x-direction when the two economies are isolated.

Supposing that γ_1 and γ_2 are small in absolute value, we impose

$$G^2_1\left(\frac{1}{2}, y\right) < m_1 + \varepsilon_d, \quad G^2_1(M_1 - \varepsilon_u, y) \geq M_1 - \varepsilon_u, \quad \forall y \in \bar{J}_1, \tag{5.7}$$

so that $S := \left\{\frac{1}{2}\right\} \times [m_1 + \varepsilon_d, M_1 - \varepsilon_u]$ (depicted in yellow in Fig. 6 (b)) is mapped by G^2_1 on the left of $\mathscr{Q}^-_r$ (depicted in brown in Fig. 6 (b)), while $\mathscr{Q}^-_\ell$ (depicted in red in Fig. 6 (b)), and thus $\mathscr{Q}^-_r$, are mapped by G^2_1 on the right of $\mathscr{Q}$, recalling the definitions in (5.2). Since in the present scenario $\gamma_1 = 0.1$ and $\gamma_2 = 0.2$, in regard to the first condition in (5.7), we notice that $G^2_1\left(\frac{1}{2}, y\right)$ is decreasing on $\bar{J}_1$ because $\frac{d}{dy} G^2_1(\frac{1}{2}, y)$, which has the same expression reported in the lines below (5.5), is negative for $y > \frac{\mu_1(1-\frac{\mu_1}{2})+\mu_2}{2(\gamma_1\mu_1+\mu_2)} = -0.434$. Hence, $G^2_1\left(\frac{1}{2}, y\right) < m_1 + \varepsilon_d$ on $\bar{J}_1$ is equivalent to $G^2_1(\frac{1}{2}, m_1 + \varepsilon_d) < m_1 + \varepsilon_d$. As concerns $G^2_1(M_1 - \varepsilon_u, y) \geq M_1 - \varepsilon_u$ on $\bar{J}_1$, a study of the sign of $\frac{d}{dy} G^2_1(M_1 - \varepsilon_u, y) = \gamma_1\big(\mu_1(1 - 2\mu_1(M_1 - \varepsilon_u)(1 - M_1 + \varepsilon_u) - 2\gamma_1 y) + \mu_2(1 - 2y)\big)$ shows that it is negative for $y > \frac{\mu_1(1-2\mu_1(M_1-\varepsilon_u)(1-M_1+\varepsilon_u))+\mu_2}{2(\gamma_1\mu_1+\mu_2)} = 0.150$, and thus the second inequality in (5.7) is equivalent to $G^2_1(M_1 - \varepsilon_u, M_1 - \varepsilon_u) \geq M_1 - \varepsilon_u$. We stress that both the found conditions are fulfilled since $G^2_1(\frac{1}{2}, m_1 + \varepsilon_d) = 0.126 < m_1 + \varepsilon_d = 0.174$ and $G^2_1(M_1 - \varepsilon_u, M_1 - \varepsilon_u) = 0.818 > M_1 - \varepsilon_u = 0.788$.

Dealing now with the compressive, vertical direction, for the time being with $\gamma_1 = \gamma_2 = 0$, since $\mu_2 = 1.7$, like with the first parameter set it happens that $g^2_{\mu_2}(y)$ admits a maximum point in $y = \frac{1}{2}$ and two minimum points in the endpoints of $\bar{J}_1$. More precisely, recalling that $\frac{1}{2} - (m_1 + \varepsilon_d) = 0.326 > M_1 - \varepsilon_u - \frac{1}{2} = 0.288$ and that $g^2_{\mu_2}(y)$ is symmetric with respect to $y = \frac{1}{2}$, it holds that $g^2_{\mu_2}(m_1 + \varepsilon_d) < g^2_{\mu_2}(M_1 - \varepsilon_u)$. Thus, to witness a contraction for G^2 along the y-direction when the

two economies are isolated, like with the first parameter set, in addition to $g^2_{\mu_2}(\frac{1}{2}) < M_1 - \varepsilon_u$, we impose $g^2_{\mu_2}(m_1+\varepsilon_d) > m_1+\varepsilon_d$, which implies $g^2_{\mu_2}(M_1-\varepsilon_u) > m_1+\varepsilon_d$.
Hence, supposing that γ_1 and γ_2 are positive but small, we impose again the conditions in (5.6), which however have to be checked in relation to the new parameter configuration. As concerns $G^2_2(x, m_1+\varepsilon_d) \geq m_1+\varepsilon_d$ on $\bar{J}_1$, we have seen just after (5.6) that $G^2_2(x, m_1+\varepsilon_d)$ has a maximum point in $x = \frac{\mu_2(1-2\mu_2(m_1+\varepsilon_d)(1-m_1-\varepsilon_d))+\mu_1}{2(\mu_1+\gamma_2\mu_2)}$, that now coincides with $x = 0.563$, while the minimum points are located in the endpoints of $\bar{J}_1$. In particular, since $G^2_2(m_1+\varepsilon_d, m_1+\varepsilon_d) = 0.456 < G^2_2(M_1-\varepsilon_u, m_1+\varepsilon_d) = 0.540$, it holds that $G^2_2(x, m_1+\varepsilon_d) \geq m_1+\varepsilon_d$ on $\bar{J}_1$ is equivalent to $G^2_2(m_1+\varepsilon_d, m_1+\varepsilon_d) \geq m_1+\varepsilon_d$. Finally, considering $G^2_2\left(x, \frac{1}{2}\right) \leq M_1-\varepsilon_u$ for every $x \in \bar{J}_1$, we have already seen that a study of the sign of $\frac{d}{dx}G^2_2\left(x, \frac{1}{2}\right)$ shows that $G^2_2\left(x, \frac{1}{2}\right)$ has a maximum point in $x = x_M := \frac{\mu_2(1-\frac{\mu_2}{2})+\mu_1}{2(\mu_1+\gamma_2\mu_2)}$, that now coincides with $x = 0.490$. Thus, the second condition in (5.6) is equivalent to $G^2_2\left(x_M, \frac{1}{2}\right) \leq M_1-\varepsilon_u$. The derived conditions are satisfied in the considered framework, since $G^2_2(m_1+\varepsilon_d, m_1+\varepsilon_d) = 0.456 > m_1+\varepsilon_d = 0.174$ and $G^2_2\left(x_M, \frac{1}{2}\right) = 0.626 < M_1-\varepsilon_u = 0.788$.

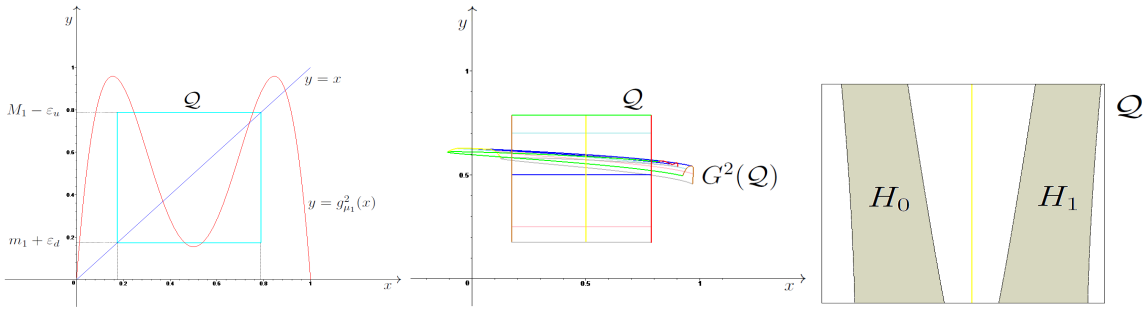

(a) (b) (c)

FIG. 6. For $\mu_1 = 3.832$, $\mu_2 = 1.7$, $\gamma_1 = 0.1$ and $\gamma_2 = 0.2$, we find in (b) a confirmation that the stretching relations in (5.3) are fulfilled for G^2, with G in (3.4), and for the square $\mathcal{Q} := \bar{J}_1 \times \bar{J}_1 = [0.174, 0.788] \times [0.174, 0.788]$ depicted in (a) and oriented as in (5.2), with H_0 and H_1 defined as in (5.4) and drawn in (c).

The analysis above is meant to give an idea of the variety in the conditions (cf. (5.5), (5.6), (5.7), and what they are equivalent to in the various frameworks) that need to be imposed in order to apply the SAP method according to the considered parameter configuration, despite the similarity between the geometry in Figs. 5 and 6. The horseshoe shape of $G^2(\mathcal{Q})$ therein is common to the chaotic attractors that emerge in the two investigated scenarios and that are illustrated in Fig. 7 (a) and (b), respectively, where the initial conditions are $x(0) = 0.7$ and $y(0) = 0.2$. We stress that, to the best of our knowledge, the ones provided above are the first applications of the SAP

method to two-dimensional discrete-time frameworks in which chaotic attractors emerge. Namely, according to Theorem II.1, if the SAP relations in (2.2) are satisfied for a certain map F, there exists a nonempty invariant set on which the function is chaotic, but nothing can be inferred about the attractiveness of the chaotic set in general,[73] and we have to rely on numerical simulations to investigate such feature. In the considered frameworks, the theoretical results obtained for G^2 are supported by the performed simulative exercises, which highlight the presence of the chaotic attractors in Fig. 7 when the SAP method is applicable.

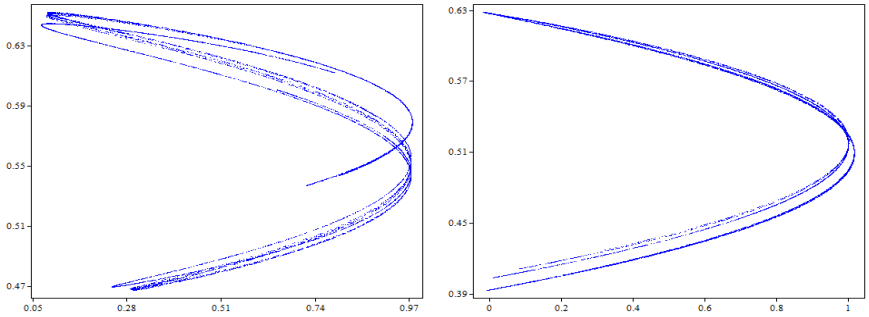

(a) (b)

FIG. 7. For G^2, with G in (3.4), we show in (a) the chaotic attractor corresponding to $\mu_1 = 3.96$, $\mu_2 = 2$, $\gamma_1 = -0.025$, $\gamma_2 = 0.16$ and in (b) the chaotic attractor corresponding to $\mu_1 = 3.832$, $\mu_2 = 1.7$, $\gamma_1 = 0.1$, $\gamma_2 = 0.2$.

We conclude by remarking that, due to the formulation of the 3D setting described at the end of Sec. IV, the three-dimensional version of the SAP method (cf. Definition 2.1 in[8] for the SAP relation between oriented 3D-rectangles, called oriented parallelepipeds therein, as well as Theorem 2.1 in[8], and the comments below it) can be easily applied to the second iterate of $\widehat{G}$ in (4.10) on the cube $\mathscr{C} := \bar{J}_1 \times \bar{J}_1 \times \bar{J}_1 = [0.124, 0.870] \times [0.124, 0.870] \times [0.124, 0.870]$, when modifying the first parameter configuration considered above for G^2, and on $\mathscr{C} = [0.174, 0.788] \times [0.174, 0.788] \times [0.174, 0.788]$, perturbing the second parameter set. In particular, it is possible to choose parameter sets with $\mu_i < 4$ for $i \in \{1,2,3\}$, so that chaotic attractors can emerge by dealing with the dynamical system generated by $\widehat{G}^2$. For instance, we could start from the two parameter configurations considered above and take $\mu_3 < 2$ close or equal to μ_2, $\gamma_{11} = \gamma_1$, $\gamma_{21} = \gamma_2$, γ_{31} close or equal to γ_2, as well as small, positive or negative, values for γ_{i2}, $i \in \{1,2,3\}$, so that $\widehat{G}^2$, which in this way is a three-dimensional perturbation of G^2, produces an expansion along the x-direction, and a contraction along the y- and z-directions. A different possibility consists in imposing symmetry between the second and the third components of $\widehat{G}^2$, by choosing $\mu_2 = \mu_3$, as

well as $\gamma_{11} = \gamma_{12} = \frac{\gamma_1}{2}$, $\gamma_{i1} = \gamma_{i2} = \frac{\gamma_2}{2}$, for $i \in \{2,3\}$. The numerical exercises we performed confirm that, starting from both the above considered parameter configurations, each solution is successful in view of applying the SAP method to $\widehat{G}^2$, witnessing chaotic attractors in the simulations. For brevity's sake, we do not show the results in all four cases, illustrating in Fig. 8 the effect of the symmetry strategy when dealing with the first parameter set and in Fig. 9 the effect of the perturbation strategy with reference to the second parameter set. The chaotic attractors in Figs. 8 and 9 are obtained with $x(0) = 0.7$, $y(0) = 0.2$ and $z(0) = 0.3$ as initial conditions. Similar to what observed above for the two-dimensional settings, we recall that, for the 3D discrete-time applications of the SAP method provided in the literature (see[7,8]), no chaotic attractors emerged, since in those frameworks the SAP technique was applied to the first, rather than to the second, iterate of the map generating the dynamics.

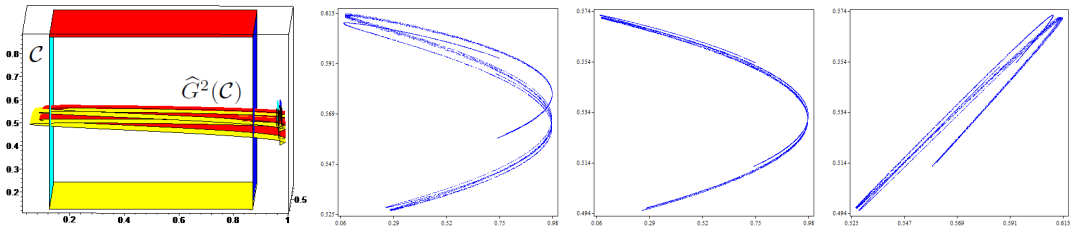

(a) (b) (c) (d)

FIG. 8. For $\widehat{G}$ in (4.10) with $\mu_1 = 3.96$, $\mu_2 = 2$, $\mu_3 = 1.8$, $\gamma_{11} = \gamma_{12} = -0.012$, $\gamma_{21} = \gamma_{22} = \gamma_{31} = \gamma_{32} = 0.08$, and the cube $\mathscr{C} := \bar{J}_1 \times \bar{J}_1 \times \bar{J}_1 = [0.124, 0.870] \times [0.124, 0.870] \times [0.124, 0.870]$, we show in (a) that $\widehat{G}^2(\mathscr{C})$, thanks to its horseshoe shape, crosses $\mathscr{C}$ horizontally twice, so that it can be proven that the 3D version of the SAP method is applicable to deduce the existence of chaos. We used the same color to draw suitable faces of $\mathscr{C}$ and their image through $\widehat{G}^2$. Keeping the parameter configuration unchanged, we show the projections, in (b) onto the *xy*-plane, in (c) onto the *xz*-plane and in (d) onto the *yz*-plane, of the corresponding chaotic attractor.

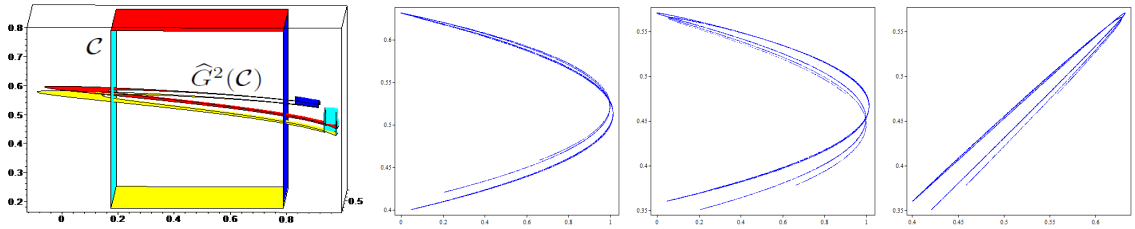

(a) (b) (c) (d)

FIG. 9. For $\widehat{G}$ in (4.10) with $\mu_1 = 3.832$, $\mu_2 = 1.7$, $\mu_3 = 1.5$, $\gamma_{11} = 0.1$, $\gamma_{12} = -0.01$, $\gamma_{21} = 0.2$, $\gamma_{22} = 0.01$, $\gamma_{31} = 0.2$, $\gamma_{32} = -0.01$, and the cube $\mathscr{C} := \bar{J}_1 \times \bar{J}_1 \times \bar{J}_1 = [0.174, 0.788] \times [0.174, 0.788] \times [0.174, 0.788]$, we show in (a) that $\widehat{G}^2(\mathscr{C})$ crosses $\mathscr{C}$ horizontally twice, so that it can be proven that the 3D version of the SAP method is applicable to deduce the existence of chaos. For the same parameter configuration, we show the projections, in (b) onto the *xy*-plane, in (c) onto the *xz*-plane and in (d) onto the *yz*-plane, of the corresponding chaotic attractor.

VI. CONCLUSION

In the present work we have shown how to apply the Stretching Along the Paths (SAP) method to prove the existence of chaotic dynamics for the 2D discrete-time model considered in[1], composed of two logistic maps, coupled by linear terms. As we have seen, the SAP technique, being topological in nature, does not require any differentiability condition. Moreover, it does not call for a direct proof of chaos according to one of the many existing definitions, which are often difficult, or impossible to handle in practical contexts.

In greater detail, along the manuscript, after determining the parameter conditions that ensure the emergence of chaotic dynamics when applying the SAP method to the first iterate of the map associated with the system considered in[1], we applied the SAP method to the second iterate of the same map in order to weaken those conditions, both in regard to the sign and the variation range of the parameters involved. Furthermore, the application of the SAP method to the second iterate of the map generating the dynamics allowed us to obtain a good agreement with the numerical simulations, that confirm the presence of a chaotic attractor under the conditions derived for the applicability of the SAP technique to the second iterate of the map, but not to the first iterate, in which case chaotic sets are not attractive. Namely, in general the SAP method ensures the existence of chaotic sets, but not their attractiveness, as discussed in[6]. To the best of our knowledge, the one we provided is the first two-dimensional discrete-time application of the SAP technique in

which numerical simulations highlight the presence of a chaotic attractor.
Since, as shown at the end of Sec. V, the same agreement between theoretical and simulative results occurs also with the 3D version of the considered model, composed by three coupled logistic maps, just when dealing with the second iterate of the function generating the dynamics, it would be interesting to understand whether, considering the second iterate of the maps associated with the 2D settings in[6] and with the 3D frameworks in[7,8], numerical simulations would confirm the presence of chaotic attractors when the model parameters satisfy the conditions for the applicability of the SAP method, recalling that in those contexts no chaotic attractors emerged when the SAP technique was applied to the first iterate of the map generating the dynamics. We will perform such investigation in a future work.

AUTHOR DECLARATIONS

Funding Information This research did not receive any specific grant.

Conflict of Interest The authors have no conflicts to disclose.

Author Contributions

Alessio Bosisio: formal analysis (equal); investigation (equal); writing - review and editing (equal).
Ahmad Naimzada: conceptualization (lead); software (equal); writing - review and editing (equal).
Marina Pireddu: methodology (lead); formal analysis (equal); investigation (equal); software (equal); investigation (equal); writing - original draft (lead); writing - review and editing (equal).

DATA AVAILABILITY

Data sharing is not applicable to this article as no new data were created or analyzed in this study.

ACKNOWLEDGMENTS

The authors thank the anonymous Reviewers for the helpful and valuable comments.

REFERENCES

[1]S. Yousefi, Y. Maistrenko, and S. Popovych, "Complex dynamics in a simple model of interdependent open economies," Discrete Dyn. Nat. Soc. **5**, 161–177 (2000).

[2]D. Papini and F. Zanolin, "On the periodic boundary value problem and chaotic-like dynamics for nonlinear Hill's equations," Adv. Nonlinear Stud. **4**, 71–91 (2004).

[3]D. Papini and Zanolin, "Fixed points, periodic points, and coin-tossing sequences for mappings defined on two-dimensional cells," Fixed Point Theory Appl. **2004**, 113–134 (2004).

[4]M. Pireddu and F. Zanolin, "Cutting surfaces and applications to periodic points and chaotic-like dynamics," Topol. Methods Nonlinear Anal. **30**, 279–319 (2007), Topol. Methods Nonlinear Anal. **33**, 395 (2009), erratum.

[5]C. Mira, L. Gardini, A. Barugola, and J.-C. Cathala, *Chaotic Dynamics in Two-Dimensional Noninvertible Maps* (World Scientific, Singapore, 1996).

[6]A. Medio, M. Pireddu, and F. Zanolin, "Chaotic dynamics for maps in one and two dimensions: a geometrical method and applications to economics," Int. J. Bifurc. Chaos Appl. Sci. Eng. **19**, 3283–3309 (2009).

[7]M. Pireddu, "Chaotic dynamics in three dimensions: A topological proof for a triopoly game model," Nonlinear Anal. Real World Appl. **25**, 79–95 (2015).

[8]M. Pireddu, "A topological proof of chaos for two nonlinear heterogeneous triopoly game models," Chaos **26**, 083106 (2016).

[9]M. Pireddu and F. Zanolin, "Chaotic dynamics in the Volterra predator-prey model via linked twist maps," Opuscula Mathematica **28/4**, 567–592 (2008).

[10]A. Margheri, C. Rebelo, and F. Zanolin, "Chaos in periodically perturbed planar Hamiltonian systems using linked twist maps," J. Differ. Equ. **249**, 3233–3257 (2010).

[11]P. G. Barrientos, J. A. Rodríguez, and A. Ruiz-Herrera, "Chaotic dynamics in the seasonally forced SIR epidemic model," J. Math. Biol. **75**, 1655–1668 (2017).

[12]K. Burns and H. Weiss, "A geometric criterion for positive topological entropy," Comm. Math. Phys. **172**, 95–118 (1995).

[13]J. Kennedy and J. A. Yorke, "Topological horseshoes," Trans. Amer. Math. Soc. **353**, 2513–2530 (2001).

[14]K. Kaneko, "Transition from torus to chaos accompanied by frequency lockings with symmetry breaking: In connection with the coupled-logistic map," Prog. Theor. Phys. **69**, 1427–1442

(1983).

[15]J.-M. Yuan, M. Tung, D. H. Feng, and L. M. Narducci, "Instability and irregular behavior of coupled logistic equations," Phys. Rev. A **28**, 1662–1666 (1983).

[16]T. Hogg and B. A. Huberman, "Generic behavior of coupled oscillators," Phys. Rev. A **29**, 275–281 (1984).

[17]H. Sakaguchi and K. Tomita, "Bifurcations of the coupled logistic map," Prog. Theor. Phys. **78**, 305–315 (1987).

[18]See[78] for an introduction to dynamical properties of the 1D logistic map.

[19]Y. L. Maistrenko, V. L. Maistrenko, A. Popovich, and E. Mosekilde, "Transverse instability and riddled basins in a system of two coupled logistic maps," Phys. Rev. E **57**, 2713–2724 (1998).

[20]A. Jakobsen, "Symmetry breaking bifurcations in a circular chain of n coupled logistic maps," Phys. D **237**, 3382–3390 (2008).

[21]N. Romero, J. Silva, and R. Vivas, "On a coupled logistic map with large strength," J. Math. Anal. Appl. **415**, 346–357 (2014).

[22]T. E. Vadivasova, G. I. Strelkova, S. A. Bogomolov, and V. S. Anishchenko, "Correlation analysis of the coherence-incoherence transition in a ring of nonlocally coupled logistic maps," Chaos **26**, 093108 (2016).

[23]P. Chandran, R. Gopal, V. K. Chandrasekar, and N. Athavan, "Chimera states in coupled logistic maps with additional weak nonlocal topology," Chaos **29**, 053125 (2019).

[24]A. Mareno and L. Q. English, "Flip and Neimark-Sacker bifurcations in a coupled logistic map system," Discrete Dyn. Nat. Soc. **2020**, 4103606 (2020).

[25]X.-Y. Yao, X.-F. Li, J. Jiang, and A. Y. T. Leung, "Codimension-one and -two bifurcation analysis of a two-dimensional coupled logistic map," Chaos Solitons Fractals **164**, 112651 (2022).

[26]I. Bashkirtseva and L. Ryashko, "Chaotic transients, riddled basins, and stochastic transitions in coupled periodic logistic maps," Chaos **31**, 053101 (2021).

[27]S. M. Salman, A. M. Yousef, and A. A. Elsadany, "Dynamic behavior and bifurcation analysis of a deterministic and stochastic coupled logistic map system," Int. J. Dyn. Control **10**, 69–85 (2022).

[28]A. D. Deshmukh, N. D. Shambharkar, and P. M. Gade, "Effect of a mode of update on universality class for coupled logistic maps: directed Ising to Ising class," Int. J. Bifurc. Chaos Appl. Sci. Eng. **31**, 2150042 (2021).

[29]N. D. Shambharkar, A. D. Deshmukh, and P. M. Gade, "Transition to fully or partially arrested state in coupled logistic maps on a ladder," Int. J. Bifurc. Chaos Appl. Sci. Eng. **31**, 2150185 (2021).

[30]V. Voutsa, M. Papadopoulos, V. Papadopoulou Lesta, and M.-T. Hütt, "The attractor structure of functional connectivity in coupled logistic maps," Chaos **33**, 083147 (2023).

[31]S. Smale, "Diffeomorphisms with many periodic points," in *Differential and Combinatorial Topology: A Symposium in Honor of Marston Morse* (Princeton University Press, Princeton, 1965) pp. 63–80.

[32]S. Wiggins, *Introduction to Applied Nonlinear Dynamical Systems and Chaos. Second Edition. Texts in Applied Mathematics* (Springer, New York, NY, 2003).

[33]On the other hand, the SAP technique seems to be not easily applicable to frameworks in which the system complexity emerges after a Neimark-Sacker bifurcation. A more detailed investigation of such kind of frameworks will be performed in order to confirm or discard this impression.

[34]A. Pascoletti and F. Zanolin, "Example of a suspension bridge ODE model exhibiting chaotic dynamics: A topological approach," J. Math. Anal. Appl. **339**, 1179–1198 (2008).

[35]M. Pireddu, "Chaotic dynamics in the presence of medical malpractice litigation: A topological proof via linked twist maps for two evolutionary game theoretic contexts," J. Math. Anal. Appl. **501**, 125224 (2021).

[36]M. Pireddu, "A proof of chaos for a seasonally perturbed version of Goodwin growth cycle model: linear and nonlinear formulations," Axioms **12**, 344 (2022).

[37]A. Ruiz-Herrera and F. Zanolin, "An example of chaotic dynamics in 3D systems via stretching along paths," Annali di Matematica **193**, 163–185 (2014).

[38]A. Ruiz-Herrera and F. Zanolin, "Horseshoes in 3D equations with applications to Lotka-Volterra systems," NoDEA Nonlinear Differ. Equ. Appl. **22**, 877–897 (2015).

[39]As we shall explain in Sec. II, when applied to 1D frameworks the SAP relation coincides with the classical covering relation considered e.g. in[56], and it can thus be viewed as an extension of the latter in general.

[40]A. Naimzada and F. Tramontana, "Two different routes to complex dynamics in an heterogeneous triopoly game," J. Difference Equ. Appl. **21**, 553–563 (2015).

[41]E. M. Elabbasy, H. N. Agiza, and A. A. Elsadany, "Analysis of nonlinear triopoly game with heterogeneous players," Comput. Math. Appl. **57**, 488–499 (2009).

[42]F. Tramontana and A. A. Elsadany, "Heterogeneous triopoly game with isoelastic demand function," Nonlinear Dyn. **68**, 187–193 (2012).

[43]P. Reichlin, "Equilibrium cycles in an overlapping generations economy with production," J. Econ. Theory **40**, 89–102 (1986).

[44]A. Medio, *Chaotic Dynamics. Theory and Applications to Economics* (Cambridge University Press, Cambridge, 1992).

[45]H. N. Agiza and A. A. Elsadany, "Chaotic dynamics in nonlinear duopoly game with heterogeneous players," Appl. Math. Comput. **149**, 843–860 (2004).

[46]M. Pireddu and F. Zanolin, "Some remarks on fixed points for maps which are expansive along one direction," Rend. Istit. Mat. Univ. Trieste **39**, 245–274 (2007).

[47]A. Pascoletti, M. Pireddu, and F. Zanolin, "Multiple periodic solutions and complex dynamics for second order ODEs via linked twist maps," Electron. J. Qualitative Theory Differ. Equ., Proc. 8'th Coll. Qualitative Theory Differ. Equ. **14**, 1–32 (2008).

[48]We stress that such left/right, down/up names are not binding from a geometric viewpoint, as it should be clear e.g. from Fig. 1, where $\mathscr{B}_\ell^-$ and $\mathscr{B}_r^-$ for the generalized rectangle $\mathscr{B}$ are the lower and the upper sides, respectively, as well as from Figs. 5 (b) and 6 (b) in Sec. V, in relation to which we selected as left and right sides of $\mathscr{Q}$ the (inverted) sets in (5.2). A similar remark concerns the choice of focusing in Definition II.1 on paths joining the left and the right sides of a generalized rectangle $\mathscr{A}$. Indeed, the choice made is consistent with our applications in Sec. IV and Sec. V, where, to fix ideas, we will assume that the expansion occurs along the x-direction. However, considering in Definition II.1 paths connecting the down and the up sides of $\mathscr{A}$ would work as well, since the homeomorphism H defining $\mathscr{A}$ could be composed with the permutation on two elements, without modifying its image set.

[49]We remark that, if $\mathscr{A} = \mathscr{B}$ but the orientation changes for the generalized rectangle when it is considered as a subset of the domain of the map F or as a subset of its codomain, Theorem 2.1 in[6] does not apply anymore and F may possibly have no fixed points. A planar example can be easily obtained following the idea in Figure 4 in[80], where 3D cylindrical sets, named $\mathscr{M}$ and $\mathscr{N}$, are illustrated.

[50]U. Kirchgraber and D. Stoffer, "On the definition of chaos," Z. Angew. Math. Mech. **69**, 175–185 (1989).

[51]J. Kennedy, S. Koçak, and J. A. Yorke, "A chaos lemma," Amer. Math. Mon. **108**, 411–423 (2001).

[52]This occurs for instance in Fig. 3, where the involved map is G in (3.4) and the disjoint compact sets are called K_0 and K_1. On the other hand, in Fig. 1, where however $\mathscr{A} \neq \mathscr{B}$, the stretching relation $(K_i, F) : \widetilde{\mathscr{A}} \overset{\sim}{\Rightarrow} \widetilde{\mathscr{B}}$ cannot be fulfilled with respect to two or more pairwise disjoint compact subsets K_i of $\mathscr{A}$. Namely, among the three red sets obtained in Fig. 1 as intersection between $\mathscr{B}$ and $F(\mathscr{A})$, only the middle one completely crosses $\mathscr{B}$ joining its left and right sides. Hence, the same is true when looking at the intersection between $\mathscr{B}$ and the image through F of any path γ in $\mathscr{A}$ linking $\mathscr{A}_\ell^-$ and $\mathscr{A}_r^-$, so that γ admits a unique subpath ν with $F(\nu)$ joining in $\mathscr{B}$ its left and right sides. Thus, in Fig. 1 there exists just one compact set $K \subset \mathscr{A}$, containing $\overline{\nu}$, such that $(K, F) : \widetilde{\mathscr{A}} \overset{\sim}{\Rightarrow} \widetilde{\mathscr{B}}$.

[53]The notation $\Sigma_2^{\oplus}$ is employed rather than the more common Σ_2^+, because the latter could be confused with the one introduced to denote the down and the up sides in relation to oriented rectangles.

[54]R. L. Adler, A. G. Konheim, and M. H. McAndrew, "Topological entropy," Trans. Amer. Math. Soc. **114**, 309–319 (1965).

[55]We stress that, as noticed by one of the Reviewers, the novelty of the SAP method, i.e., of Definition II.1 and Theorem II.1, with respect to the original Smale horseshoe framework (see Proposition 2.4.1 and Section 5.1 in[76]) arises when, like it happens in the applicative contexts considered in the present paper, F in Theorem II.1 is not injective on the set $K := K_0 \cup K_1$. Namely, if F were injective on K, so that in particular $F(K_0) \cap F(K_1) = \emptyset$, then $\hat{Y} := \bigcap_{n=-\infty}^{\infty} F^{-n}(K)$ would contain a nonempty, compact and invariant set $\hat{X}$ such that the map F restricted to it would be conjugate or semiconjugate - rather than to the one-sided Bernoulli shift on two symbols, as described in (ii) of Theorem II.1 - to the *two-sided* Bernoulli shift on two symbols, i.e., to $\sigma : \Sigma_2 \to \Sigma_2$, $\sigma((s_i)_i) := (s_{i+1})_i$, $\forall i \in \mathbb{Z}$, where $\Sigma_2 := \{0,1\}^{\mathbb{Z}}$, like it occurs with the classical Smale horseshoe construction.

[56]L. Block, J. Guckenheimer, M. Misiurewicz, and L. S. Young, "Periodic points and topological entropy of one-dimensional maps," in *Global Theory of Dynamical Systems (Proc. Internat. Conf., Northwestern Univ., Evanston, Ill., 1979). Lecture Notes in Mathematics*, Vol. 819, edited by Z. Nitecki and C. Robinson (Springer, Berlin, Heidelberg, 1980) pp. 18–34.

[57]A. Naimzada and M. Pireddu, "Dynamic behavior of product and stock markets with a varying degree of interaction," Econ. Model. **41**, 191–197 (2014).

[58]A. Naimzada and M. Pireddu, "Real and financial interacting markets: A behavioral macromodel," Chaos, Solitons Fractals **77**, 111–131 (2015).

[59]F. Cavalli, A. Naimzada, N. Pecora, and M. Pireddu, "Agents' beliefs and economic regimes polarization in interacting markets," Chaos **28**, 055911 (2018).

[60]F. Cavalli, A. Naimzada, and N. Pecora, "A stylized macro-model with interacting real, monetary and stock markets," J. Econ. Interact. Coord. **17**, 225–257 (2022).

[61]Namely, we could rewrite the conditions in (4.6) respectively as $G_1(\mathscr{R}_\ell^-) \leq 0$, $G_1(\mathscr{R}_r^-) \leq 0$, so that the left and the right sides of $\mathscr{R}$ are mapped by G_1 on the left of $\mathscr{R}_\ell^-$ (i.e., inside the strip $(-\infty, 0] \times \mathbb{R}$), and $G_1(S) > 1$, meaning that the vertical segment $S := \left\{\frac{1}{2}\right\} \times [0, c]$, lying in the middle of $\mathscr{R}$, is mapped by G_1 on the right of $\mathscr{R}_r^-$ (i.e., inside the strip $(1, +\infty) \times \mathbb{R}$). Notice that the latter inequality needs to be strict in order to ensure that the compact sets K_0 and K_1 to be defined in (4.8) are disjoint. A similar remark applies to the first inequality in (5.5) and in (5.7), too.

[62]Indeed, the conditions in (4.7) ensure that $G_2(\mathscr{R})$ is contained in the infinite horizontal strip $\mathbb{R} \times [0, c]$, that contains $\mathscr{R}$, too.

[63]The parameter conditions in (4.2)–(4.4) modified by interchanging therein μ_1 with μ_2 and γ_1 with γ_2 would imply that G is instead expansive along the y-direction and compressive along the x-direction, due to the symmetric expressions for G_1 and G_2.

[64]Namely, according to the results in Sec. 5 in[4], Theorem II.1 holds true when dealing with oriented N-dimensional rectangles for any $N \geq 3$.

[65]The present formulation, although in a variant encompassing delays, has been considered in[77]. See e.g.[82] for a different formulation of a system composed of three coupled logistic maps without delays.

[66]See Definition 5.3 in[4] for the SAP relation between oriented N-dimensional rectangles, with $N \geq 3$, and, more specifically, Definition 2.1 in[8] for the 3D framework.

[67]We stress that such technique bears some resemblance to the one described in[58], where however the focus is on the channels that allow to transmit the instability between the real and the financial sectors, rather than on chaotic dynamics in a more formal way. As underlined in Sec. III, due to the different model formulations, the linking parameters in[58] could vary just in the interval $[0, 1]$, while in the here analyzed framework there are no a priori limitations on their sign and on their variability range, because of their economic interpretation.

[68]Notice that, despite the overall similarity between our Fig. 4 and Fig. 2 in[6], the intervals highlighted in the two pictures do not coincide.

[69]Since Φ has to map the compact set Z into itself, in the framework described in Theorem II.1 the dynamical system to be considered is given by (X,F), where X is the compact invariant set.

[70]We stress that, even if a weak inequality is present in (5.5), we need to impose all strict inequalities in the construction about $g^2_{\mu_1}(x)$ because the conditions on G^2_1 in (5.5) are obtained, by a continuity argument, for sufficiently small (in modulus) values of γ_1 and γ_2, starting from the conditions on $g^2_{\mu_1}(x)$. A similar remark applies to the relationship between the weak inequalities in (5.6) and the strict inequalities in the construction about $g^2_{\mu_2}(y)$ in the preceding lines.

[71]Notice that if (5.5) and (5.6) are fulfilled for certain values of γ_1 and γ_2 (and this can be checked graphically or analytically), then, by construction, the SAP method can be successfully applied to G^2 on $\mathscr{Q}$, not only for those values of the coupling parameters, but also for any pair of values for γ_1 and γ_2 that are smaller in modulus with respect to the original ones, when keeping their signs unchanged. Hence, in what follows, we will verify that the stretching relations in (5.3) are satisfied for $\gamma_1 = -0.025$ and $\gamma_2 = 0.16$, so that they then hold for any value of $-0.025 \leq \gamma_1 \leq 0 \leq \gamma_2 \leq 0.16$.

[72]In order not to overburden notation, in what follows we will use the same symbols as with the first parameter set.

[73]See[6] for a discussion on the attractiveness of chaotic sets in the presence of backward dynamics, based on the Inverse Limit Approach, described in[79].

[74]J. Auslander and J. A. Yorke, "Interval maps, factors of maps, and chaos," Tôhoku Math. J. **32**, 177–188 (1980).

[75]W. A. Brock and C. H. Hommes, "A rational route to randomness," Econometrica **65**, 1059–1095 (1997).

[76]J. Guckenheimer and P. Holmes, *Nonlinear Oscillations, Dynamical Systems, and Bifurcations of Vector Fields. Applied Mathematical Sciences* (Springer, New York, NY, 1986).

[77]S. Hidaka, N. Inaba, M. Sekikawa, and T. Endo, "Bifurcation analysis of four-frequency quasi-periodic oscillations in a three-coupled delayed logistic map," Phys. Lett. A **379**, 664–668 (2015).

[78]R. M. May, "Simple mathematical models with very complicated dynamics," Nature **261**, 459–467 (1976).

[79]A. Medio and B. Raines, "Backward dynamics in economics. The inverse limit approach," J. Econ. Dyn. Control **31**, 1633–1671 (2007).

[80]M. Pireddu and F. Zanolin, "Fixed points for dissipative-repulsive systems and topological dynamics of mappings defined on n-dimensional cells," Adv. Nonlinear Stud. **5**, 411–440 (2005).

[81]C. Robinson, *Dynamical Systems. Stability, Symbolic Dynamics, and Chaos. Second edition. Studies in Advanced Mathematics* (CRC Press, Boca Raton, FL, 1999).

[82]K. Satoh, "Numerical study on a coupled logistic map as a simple model for three competing species," J. Phys. Soc. Japan **60**, 1533–1540 (1991).

[83]P. Zgliczyński and M. Gidea, "Covering relations for multidimensional dynamical systems," J. Differ. Equ. **202**, 32–58 (2004).